

# The Vector Mesonic Spectrum of a Large N QCD Model in String Theory

Olivier Trottier

Master of Science

Physics Department

McGill University

Montreal, Québec

2013-08-15

As partial fulfilment of the requirements of the degree of Master of Science

©2013 Olivier Trottier

## DEDICATION

I dedicate this thesis to my father Marc Trottier and my mother Maude Gagnon. While my father would nourish my childhood dreams with science-fiction and encourage me to boldly go where no one has gone before, my mother would read me scientific encyclopaedias and nurture my Charlie Brown curiosity.

Merci pour votre amour.

## ACKNOWLEDGEMENTS

In the large  $N$  limit, I am  $N$  times thankful to my supervisor Keshav Dasgupta who was always available to answer my questions on string theory. I am also grateful for his advice on the inner workings of academia.

I wish to thank my collaborators and friends Long Chen, Fang Chen, Mohammed Mia and Michael Richard who gave me valuable insights that helped perform my calculations.

## ABSTRACT

Following the holographic QCD model of Sakai and Sugimoto, we analyze the mesonic spectrum of a large  $N$  thermal QCD model in the dual string theory. After a T-dual transformation, the background of the ten-dimensional spacetime contains  $N$  D4-branes and  $N_f$  D6/ $\overline{\text{D6}}$ -branes and the internal manifold consists of a resolved-deformed conifold whose  $\psi$  direction is the analogue of the compact cycle of the Sakai-Sugimoto's geometry. Using the probe approximation, we study the DBI action of the D6-branes and, by restricting the coordinate dependence of the ten-dimensional gauge flux components  $A_M$ , we recover a four-dimensional QCD-like action. In particular, this reduced action contains mass terms of vector mesons, which are related to the Minkowski components of the gauge flux. We calculate the values of these masses and our predictions find good agreement with the experimental values.

## RÉSUMÉ

Inspiré par le modèle de mécanique chromodynamique(QCD) holographique de Sakai et Sugimoto, nous analysons, dans la limite où  $N$  est grand, le spectre mésonique d'un modèle de QCD à température finie à partir de la théorie des cordes correspondante. Après une transformation de dualité T, l'espace-temps de dix dimensions contient  $N$  D4-branes et  $N_f$  D6/ $\overline{\text{D6}}$ -branes et les dimensions enroulées consistent en une variété conique dont la dimension  $\psi$  est l'analogue de la dimension enroulée de la géométrie de Sakai-Sugimoto. En utilisant l'approximation de sonde, nous étudions l'action DBI des D6-branes et, en restreignant la dépendance des composantes du flux de jauge  $A_M$  de dix dimensions sur les coordonnées Minkowskiennes et  $\psi$ , nous retrouvons une action à quatre dimensions semblable à celle de QCD. Entre autres, cette action réduite contient des termes de masse de mésons vectoriels lesquels sont reliés aux composantes du flux de jauge. Nous calculons les valeurs de ces masses et nos prédictions sont comparables aux valeurs expérimentales.

## TABLE OF CONTENTS

	DEDICATION . . . . .	2
	ACKNOWLEDGEMENTS . . . . .	3
	ABSTRACT . . . . .	4
	RÉSUMÉ . . . . .	5
	LIST OF TABLES . . . . .	8
	LIST OF FIGURES . . . . .	9
1	Introduction . . . . .	10
2	Quantum Chromodynamics . . . . .	13
	2.1 Action . . . . .	13
	2.2 Symmetries . . . . .	14
	2.3 Particle Content . . . . .	17
	2.4 Confinement . . . . .	18
	2.5 Asymptotic Freedom . . . . .	19
3	Concepts of String Theory . . . . .	21
	3.1 Bosonic Strings . . . . .	21
	3.2 Superstrings . . . . .	24
	3.3 Type II Superstring Theories . . . . .	27
	3.4 D-Branes . . . . .	29
	3.5 Compactification . . . . .	30
	3.6 T-Duality . . . . .	31
4	Holography . . . . .	34
	4.1 Planar vs Non-Planar Diagrams . . . . .	34
	4.2 Large N Expansion . . . . .	35

4.3	AdS/CFT from the Low-Energy Spectrum Point of View . . . . .	37
4.4	AdS/CFT from the Symmetries and Parameters Point of View . .	41
5	The Sakai-Sugimoto Model . . . . .	43
5.1	Essence of the Model . . . . .	43
5.2	Successes and Limitations . . . . .	45
5.3	D8-brane Stability in the D4 Background . . . . .	48
5.4	Masses of Vector Mesons . . . . .	51
5.5	Masses of Scalar Mesons . . . . .	54
6	A UV Complete Model of Holographic QCD . . . . .	56
6.1	Main Building Blocks . . . . .	56
6.2	Successes . . . . .	58
6.3	Gauge Theory Picture . . . . .	59
6.4	Gravity Picture . . . . .	60
6.5	Resemblance with the Sakai-Sugimoto Model . . . . .	65
7	Mesonic Spectrum Calculations . . . . .	68
7.1	D8-Brane Metric and B-field . . . . .	68
7.2	D8-Brane Embedding . . . . .	69
7.3	D8-Brane Action with Flux . . . . .	71
7.4	Vector Mesons . . . . .	75
	7.4.1 Zeroth-Order Eigenvalue . . . . .	77
	7.4.2 Zeroth-Order Eigenfunctions . . . . .	80
	7.4.3 First-Order Eigenvalue . . . . .	83
	7.4.4 Field Identification . . . . .	83
	7.4.5 Comparison of the Mass Ratios . . . . .	85
8	Conclusion . . . . .	89
	References . . . . .	91

LIST OF TABLES

Table	page
2-1 Quantum numbers of the up and down quarks. . . . .	17
2-2 $\rho$ and $a$ mesons quantum information. . . . .	18
3-1 Type IIA vs Type IIB. . . . .	28
5-1 Brane content of the Sakai-Sugimoto model. . . . .	44
5-2 Masses of vector and scalar mesons in the Sakai-Sugimoto model. . . . .	47
5-3 Sakai-Sugimoto's predictions for ratios of mesons' masses . . . . .	55
6-1 Brane content of the MDGJ model. . . . .	60
6-2 Brane content of the $T_\psi$ -dual MDGJ model. . . . .	65
6-3 IR picture of the $T_\psi$ -dual MDGJ model. . . . .	66
7-1 Zeroth-order eigenvalues of the six lightest vector mesons in the MDGJ model. . . . .	80
7-2 Vector mesons of the MDGJ model. . . . .	85
7-3 MDGJ vs Sakai-Sugimoto predictions determining $\delta$ by fixing $R_{2/1}$ . . . . .	86
7-4 MDGJ vs Sakai-Sugimoto predictions determining $\delta$ by minimizing the vector mesons $\chi^2$ . . . . .	87

LIST OF FIGURES

<u>Figure</u>	<u>page</u>
4-1 Examples of planar and non-planar diagrams. . . . .	34
4-2 Planar and non-planar diagrams in the double-line formalism.[1] . . .	35
6-1 D7-brane configuration in the three radial regions. [2] . . . . .	63
6-2 Span of the D4-branes in the $\psi$ dimension. . . . .	67
7-1 Zeroes of $\alpha_n(0, \lambda_n)$ and $\partial_Z \alpha_n(0, \lambda_n)$ . . . . .	79
7-2 Zeroth-order eigenfunctions of the six lightest vector mesons in the MDGJ model. . . . .	81

## CHAPTER 1

### Introduction

In the 1970s, Gerard 't Hooft was analyzing the large  $N$  limit of Yang-Mills theory and his conclusions were rather unexpected as he found that Feynman diagrams had the topology of the world-sheet of a string with quarks at its ends [3]. Though this limit was deemed useful, one wouldn't think that it could be applicable to the theory of strong interactions where the number of colors is small. Inspired by his work, Juan Maldacena studied the large  $N$  limit of Yang-Mills theories from the perspective of string theory and made a ground-breaking discovery [4]. By examining the low-energy spectrum of a supersymmetric conformal large  $N$  Yang-Mills theory, he conjectured that this theory (CFT) would coincide with a theory of gravity in an Anti-de Sitter spacetime (AdS). The AdS/CFT correspondence ignited research in physics where people started studying this intriguing duality in various contexts such as quantum information theory, condensed matter physics, nuclear physics and string theory. For example, condensed matter theorists started thinking about topological insulators from a gravitational point of view using Maldacena's correspondence and derived formulas for transport coefficients [5]. The duality has also been applied to give a holographic interpretation of entanglement entropy and find its relation to black hole entropy [6]. Also, one could say that this correspondence is one more step towards finding a theory that unifies the quantum and gravitational worlds.

AdS/CFT also became very useful in studying the theory of the strong interaction, namely Quantum Chromodynamics (QCD), and this new framework to understand QCD became commonly known as AdS/QCD. In this context, one generalizes the principles of AdS/CFT to non-conformal quantum field theories aiming to probe the least controllable regime of QCD, i.e., the large-coupling limit. AdS/QCD also provides an interpretation of the confinement/deconfinement phase transition of thermal QCD and suggests a new perspective to study the quark-gluon plasma, an exotic state of matter that is incomprehensible in the pure QCD theory. String theorists [7] have managed to derive a lower bound on the shear viscosity-to-volume density of entropy ratio, which was confirmed by the Relativistic Heavy Ion Collider [8]. However, a clear holographic picture of QCD hasn't been found yet and many people [9, 10, 11] have devoted their work to find a gravity dual theory that encompasses the true nature of QCD. The work presented in this dissertation subscribes to this program and aims to improve the holographic QCD picture at the level of the mesonic spectrum. We choose to develop the holographic description of the model presented by Mohammed Mia, Keshav Dasgupta, Charles Gale and Sangyong Jeon [11]. Finding mesonic fields with correct masses in the dual gravity picture is our main objective.

In chapter 2 and 3, we introduce key aspects of the literature relevant to this study, which relates quantum chromodynamics to string theory. Chapter 4 is dedicated to explain the main idea of the AdS/CFT correspondence and give evidence that this conjecture is true. Chapter 5 presents the Sakai-Sugimoto model, which inspired us to conduct the analysis of the vector mesonic spectrum in the dual gravity

theory and predict numerical values for their masses. In chapter 6, we summarize the model in which our calculations are undertaken and show its similarities to the construction of Sakai and Sugimoto. The last chapter details the calculations of the mesonic masses before we compare them with Sakai-Sugimoto's predictions and the empirical values.

## CHAPTER 2

### Quantum Chromodynamics

Quantum Chromodynamics (QCD) is a non-abelian quantum field theory, also known as a Yang-Mills theory, whose gauge group is  $SU(3)$  and fundamental quantum fields are quarks and gluons. Quarks are fermions that possess a conserved charge named "color" (red, blue or green) as a consequence of Noether's theorem. They bound with one another to form metastable/stable particles, but can never be isolated. Gluons are the gauge bosons that mediate the color force.

#### 2.1 Action

The dynamics of quarks and gluons is summarized by the QCD Lagrangian <sup>1</sup>.

$$\mathcal{L}_{\text{QCD}} = \bar{\psi} (-i\gamma^\mu D_\mu - m) \psi - \frac{1}{2} \text{Tr}(F_{\mu\nu} F^{\mu\nu}) \quad (2.1)$$

$$D_\mu \equiv \partial_\mu - igA_\mu \quad (2.2)$$

$$F_{\mu\nu} = \partial_\mu A_\nu - \partial_\nu A_\mu + g[A_\mu, A_\nu] \quad (2.3)$$

In  $\mathcal{L}_{\text{QCD}}$ ,  $\psi$ ,  $A_\mu$ ,  $\gamma_\mu$ ,  $m$  and  $g$  represent the quark fields, the gluon fields, the 4-dimensional Dirac matrices, the quark mass and the coupling constant, respectively. Also, the Einstein convention for repeated indices is understood throughout the end

---

<sup>1</sup> The mostly + convention of the Minkowski metric  $\eta_{\mu\nu}$  will be used throughout this text.

of this dissertation unless stated otherwise. In addition to their spinor index, the quark fields possess a color index that is usually noted by a roman letter. The gluon fields are  $3 \times 3$  complex matrices, which belong to the Lie Algebra of  $SU(3)$  commonly symbolized as  $\mathfrak{su}(3)$ . Hence, identifying  $T^a (a \in \{1, \dots, 8\})$  as the generators of  $\mathfrak{su}(3)$ , we decompose  $A_\mu$  as follows:  $A_\mu = A_\mu^a T^a$ . By normalizing the generators according to  $\text{Tr}(T^a T^b) = \frac{1}{2} \delta^{ab}$  and using the structure constants  $f^{abc}$  defined by  $[T^a, T^b] = f^{abc} T^c$ , one can rewrite the Lagrangian in another common form.

$$\mathcal{L}_{\text{QCD}} = \bar{\psi}_i (-i\gamma^\mu (D_\mu)_{ij} - m(\mathbf{1})_{ij}) \psi_j - \frac{1}{4} (F_{\mu\nu}^a F^{a\mu\nu}) \quad (2.4)$$

$$(D_\mu)_{ij} \equiv \partial_\mu (\mathbf{1})_{ij} - ig A_\mu^a (T^a)_{ij} \quad (2.5)$$

$$F_{\mu\nu}^a = \partial_\mu A_\nu^a - \partial_\nu A_\mu^a + gf^{abc} A_\mu^b A_\nu^c \quad (2.6)$$

In the formulas above, we have written the color indices  $(i, j)$  explicitly for the sake of clarity.

## 2.2 Symmetries

QCD exhibits many kinds of symmetries, which we summarize in the lines below. We also describe the behavior of the dynamic fields under each symmetry transformation.

First of all, QCD possesses the Lorentz symmetry. This symmetry is manifestly displayed in the Lagrangian by the absence of free spacetime indices ( $\mu$ ). The fermionic quark fields belong to spinor representations of the Lorentz group and, as

such, they transform as follows:

$$\psi_k \rightarrow \left( e^{-\frac{i}{2} \omega_{\mu\nu} S^{\mu\nu}} \right)_{kl} \psi_l \quad (\text{for some spinor index } k \in \{1, \dots, 4\}) \quad (2.7)$$

$$S^{\mu\nu} \equiv \frac{i}{4} [\gamma^\mu, \gamma^\nu] \quad (2.8)$$

With respect to Lorentz transformations, the gluon fields are vectors, i.e., they belong to the fundamental representation of the Lorentz group [12].

$$A^\alpha \rightarrow \left( e^{-\frac{i}{2} \omega_{\mu\nu} (\mathcal{J}^{\mu\nu})} \right)_{\beta}^{\alpha} A^\beta \quad (2.9)$$

$$(\mathcal{J}^{\mu\nu})_{\alpha\beta} \equiv i (\delta^\mu_\alpha \delta^\nu_\beta - \delta^\mu_\beta \delta^\nu_\alpha) \quad (2.10)$$

As part of its definition, QCD also possesses a *local* gauge symmetry whose transformations are elements of the group  $SU(3)$ . If  $U(x)$  is a unitary  $3 \times 3$  matrix whose entries depend on the spacetime coordinate  $x^\mu$ , then, under a gauge transformation parametrized by  $U(x)$ , the quarks and gluons behave as follows:

$$\psi^c \rightarrow (U)^c_d \psi^d \quad (\text{for some color index } c \in \{1, \dots, 3\}) \quad (2.11)$$

$$A_\mu \rightarrow U A_\mu U^\dagger - i \partial_\mu (U) U^\dagger \quad (2.12)$$

One can also consider an ensemble of  $N_f$  quarks that interact with one another. In the Lagrangian, the quark field would have an extra index, commonly called a flavor index. The mass term would be enhanced to a mass matrix whose diagonal components correspond to the mass of the corresponding flavor. If all the  $N_f$  quarks have the same mass, one could interchange them by means of a  $SU(N_f)$  matrix and recover the same Lagrangian, hence the ensemble of quarks would exhibit an extra  $SU(N_f)$  symmetry.

In QCD, there are six flavors of quarks, known as *up*(u), *down*(d), *charm*(c), *strange*(s), *bottom*(b) and *top*(t). These six flavors all have different mass and the flavor symmetry is consequently broken. However, the symmetry is partially restored in an approximate meaning by noticing that the up and down quarks have similar masses ( $M_u \approx 2 \text{ MeV}$ ,  $M_d \approx 4 \text{ MeV}$  [13]). This symmetry is often called isospin symmetry since its mathematical formulation is similar to the one for spin ( $SU(2)$ ). As it is similarly done for spin, one is interested in the amount of isospin in the z-direction ( $I_3$ ) of a given particle. This quantity is intimately related to the the number of up ( $N_u$ ) and down ( $N_d$ ) quarks of a particle by the following formula:

$$I_3 = \frac{1}{2}(N_u - N_d) \quad (2.13)$$

Yet another symmetry that one may encounter in Yang-Mills theories is chiral symmetry. If one carefully chooses the representation of the Dirac matrices, which determines the transformation rule of the Dirac spinors, the matrix representing the Lorentz group generators in the spinor representation can be written in a block diagonal form whose blocks are  $2 \times 2$  matrices. With the additional massless condition, the upper two components (Left) and the lower two components (Right) of the Dirac spinors can be modified independently. Mixed with flavor symmetry, one can have chiral flavor symmetry where the left and right part of the up and down spinors put together have their respective flavor group ( $SU(2)_L \times SU(2)_R$ ) [14].

Chiral symmetry is broken in QCD by a quark condensate. According to Goldstone's theorem [15], this symmetry breaking must create goldstone bosons. For the chiral flavor symmetry breaking  $SU(2)_L \times SU(2)_R \rightarrow SU(2)$  of the up and down

quark, the bosons associated to the three broken generators are the three pions  $\pi^0, \pi^+, \pi^-$ .

### 2.3 Particle Content

The quark model proposed by QCD allows us to explain the existence of many observed particles. For this reason, it is one of the main building blocks of the Standard Model where all the hadrons are built from bound states of quarks and anti-quarks of various flavors.

The hadronic family of particles is composed of baryons and mesons. Baryons are formed by the bonding of three quarks or anti-quarks while mesons arise as the bound state of a quark and anti-quark. By knowing the quantum numbers of each flavor of quarks, one can easily derive the quantum numbers of the bound states simply by adding the quantum numbers of its quark constituents. For example, here is a table that summarizes the spin angular momentum ( $s$ ), the baryon number ( $B$ ), the isospin ( $I_3$ ), the charmness ( $C$ ), the strangeness ( $S$ ), the topness ( $T$ ) and the bottomness ( $B'$ ) of the up and down quarks.

Table 2-1: Quantum numbers of the up and down quarks.

Name	$s$	$B$	$Q$	$I_3$	$C$	$S$	$T$	$B'$
Up	$\frac{1}{2}$	$\frac{1}{3}$	$\frac{2}{3}$	$\frac{1}{2}$	0	0	0	0
Anti-Up	$\frac{1}{2}$	$-\frac{1}{3}$	$-\frac{2}{3}$	$-\frac{1}{2}$	0	0	0	0
Down	$\frac{1}{2}$	$\frac{1}{3}$	$-\frac{1}{3}$	$-\frac{1}{2}$	0	0	0	0
Anti-Down	$\frac{1}{2}$	$-\frac{1}{3}$	$\frac{1}{3}$	$\frac{1}{2}$	0	0	0	0

In our analysis of a holographic model of large N QCD, we will mostly be concerned with scalar and vector mesons that are flavorless, i.e., are only formed by bound states of up and down quarks. In particular, we will focus on the  $\rho$  and  $a$  series for which we present an overview of their quantum numbers [16].

Table 2–2:  $\rho$  and  $a$  mesons quantum information.

Name	$I_3$	P	C	J	Type
$\rho$	1	-	-	1	Vector
$a_0$	1	+	+	0	Scalar
$a_1$	1	+	+	1	Pseudovector

$P$ ,  $C$  and  $J$  stands for parity, charge conjugation and total angular momentum respectively.

## 2.4 Confinement

A unique feature of quantum chromodynamics is the linear potential between quarks. This implies that they are constantly attracted to one another regardless of the distance that separates them. In other words, an infinite energy would be required to separate them completely, which explains the impossibility to isolate quarks experimentally.

In order to find the quark potential and verify its linearity, one usually calculates the expectation value of the following Wilson loop:

$$\langle W_C \rangle = \langle \text{Tr}(e^{ig \oint_C dx^\mu A_\mu}) \rangle \quad (2.14)$$

$$= \text{Tr} \left( \int \mathcal{D}\mathcal{A} e^{-S} e^{ig \oint_C dx^\mu A_\mu} \right) \quad (2.15)$$

where  $C$  is a rectangular loop through space and time whose spatial length is  $R$  and temporal length is  $T$ . When  $T \rightarrow \infty$ , the loop corresponds to the trajectory of two charged particles (quarks in this case), which are separated by a spatial distance  $R$ . In this limit, we expect  $\langle W_C \rangle$  to behave as  $\log(\langle W_C \rangle) \sim -iET$  where  $E$  is the energy corresponding to the pair of charged particles.

If  $\log(\langle W_C \rangle) \propto RT$ , this implies that the energy of the pair grows linearly with their separation length:  $E(R) \propto R$ . In other words, the particles are confined and this behavior of the Wilson loop is called the *area law*. On the other hand, if  $\log(\langle W_C \rangle) \propto P$ , where  $P$  is the perimeter of  $C$ , the particles are not confined. In this case, the Wilson loop exhibits the *perimeter law*, which is typical of quantum electrodynamics (QED).

## 2.5 Asymptotic Freedom

One of the most important aspect of QCD is its asymptotic freedom, which was discovered conjointly by David Gross, Frank Wilczek [17] and David Politzer [18]. In a nutshell, asymptotic freedom states that the coupling constant of QCD flows to a vanishing value as one increases the energy scale  $\mu$  in the renormalization flow. This is evidenced by calculating the beta function  $\beta(g, \mu)$  of the said coupling "constant", which is found by studying the Callan-Symanzik equation [12]. The beta function

informs us about the evolution of the coupling in the following manner:

$$\mu \frac{d}{d\mu} g(\mu) = \beta(g, \mu) \tag{2.16}$$

For the particular case of QCD, the beta function of the coupling constant is *negative*. In other words, it decreases as the energy scale increases. This implies that fields in some dynamical process interact as though the coupling was small when the characteristic energy scale of the process is high (eg. inelastic scattering). This is very profound since, for high energy interactions, one needs only consider a few Feynman diagrams to obtain reasonably accurate predictions. However, the downfall of asymptotic freedom is the uncontrollable perturbative expansions of low energy processes. But all hope is not lost when one considers string theory models of QCD and uses the ubiquitous gauge/gravity dualities.

## CHAPTER 3

### Concepts of String Theory

In this section, our goal is to present an overview of the basic concepts of string theory that will be useful to understand the holographic QCD models relevant to this study. The presentation is not meant to be fully pedagogical for the sake of brevity. Plenty of thorough textbooks can be found in the literature [19, 20, 21, 22].

#### 3.1 Bosonic Strings

The starting point of string theory is to consider the relativistic dynamics of extended objects in an arbitrary spacetime of  $D$  dimensions with metric  $g_{\mu\nu}$ . The simplest of these objects is no more than a (bosonic) string. To find its dynamical evolution, one generalizes the action for point particles to obtain the Nambu-Goto action [21]:

$$S_{NG} = -T \int d^2\sigma \sqrt{-\det(h_{ab})} \tag{3.1}$$

$$h_{ab} = g_{\mu\nu} \partial_a X^\mu \partial_b X^\nu \tag{3.2}$$

where  $T$  is the string tension,  $h_{ab}$  is the induced metric on the string world-sheet and  $a, b$  refer the world-sheet parameters  $\{\sigma^0, \sigma^1\}$ . One of these parameters ( $\sigma^0 \equiv \tau \in \mathbb{R}$ ) is timelike, while the other ( $\sigma^1 \equiv \sigma \in [0, \pi]$ ) is spacelike. To simplify the quantization of the several vibrating modes of the string, one must consider an equivalent action,

namely, the Polyakov action:

$$S_P = -\frac{T}{2} \int d^2\sigma \sqrt{-h} h^{ab} \partial_a X^\mu \partial_b X_\mu \quad (3.3)$$

This action possesses various symmetries, which one can use to fix the components of the induced metric as in the static gauge. These symmetries are:

1. Invariance under Poincaré transformations.

$$\begin{aligned} X^\mu &\rightarrow (\eta^\mu{}_\nu + a^\mu{}_\nu) X^\nu + b^\mu, & a_{\mu\nu} &= -a_{\nu\mu} \\ h_{ab} &\rightarrow h_{ab} \end{aligned} \quad (3.4)$$

2. Invariance under world-sheet reparametrizations.

$$\begin{aligned} X^\mu &\rightarrow X^\mu \\ h_{ab}(\sigma^a) &\rightarrow \partial_a f^c \partial_b f^d h_{cd}(\sigma'^a), & \sigma^b &\rightarrow \sigma'^b \equiv f^b(\sigma^a) \end{aligned} \quad (3.5)$$

3. Invariance under Weyl transformations.

$$\begin{aligned} X^\mu &\rightarrow X^\mu \\ h_{ab} &\rightarrow e^{\phi(\sigma)} h_{ab} \end{aligned} \quad (3.6)$$

Upon variation of the embedding coordinates  $X^\mu$ , one finds the generalized equation of motion (EOM) for strings in a curved background, which is written in terms of

the Laplace-Beltrami operator  $\Delta$ .

$$\Delta X^\mu = -\frac{1}{\sqrt{-h}} \left( \sqrt{-h} h^{ab} \partial_b X^\mu \right) = 0 \quad (3.7)$$

Along with the EOM, one can impose three kinds of boundary conditions for  $X^\mu$  that naturally lead to three kinds of strings.

1. Periodic boundary conditions yield closed strings.

$$X^\mu(\sigma, \tau) = X^\mu(\sigma + \pi, \tau) \quad (3.8)$$

2. Dirichlet boundary conditions yield open strings.

$$X^\mu|_{\sigma=0} = C_0^\mu, \quad X^\mu|_{\sigma=\pi} = C_\pi^\mu, \quad \mu = 1, \dots, D - p - 1, \text{ (for some constants } C_0^\mu, C_\pi^\mu \text{ )} \quad (3.9)$$

3. Neumann boundary conditions yield open strings.

$$\partial_\sigma X^\mu|_{\sigma=0} = \partial_\sigma X^\mu|_{\sigma=\pi} = 0, \quad \mu = D - p, \dots, D \quad (3.10)$$

When one parametrizes the world-sheet with lightcone coordinates  $\sigma^\pm = \tau \pm \sigma$  and uses the lightcone gauge for the induced metric  $h_{ab}$ , the EOM becomes quite simple and the solution separates into a left-moving and right-moving part.

$$\partial_+ \partial_- X^\mu = 0 \quad (3.11)$$

$$\Rightarrow X^\mu(\sigma, \tau) = X_L^\mu(\sigma^+) + X_R^\mu(\sigma^-) \quad (3.12)$$

One can then consider the most general expansion that satisfies the EOM using the string center-of-mass position  $X_0^\mu$  and total momentum  $p^\mu$ .

$$X_L^\mu = \frac{1}{2}X_0^\mu + \alpha' p^\mu(\sigma^+) + i\sqrt{\frac{\alpha'}{2}} \sum_{n=-\infty, n \neq 0}^{\infty} a_n^\mu e^{-in\sigma^+} \quad (3.13)$$

$$X_R^\mu = \frac{1}{2}X_0^\mu + \alpha' p^\mu(\sigma^-) + i\sqrt{\frac{\alpha'}{2}} \sum_{n=-\infty, n \neq 0}^{\infty} \tilde{a}_n^\mu e^{-in\sigma^-} \quad (3.14)$$

When one quantizes the string modes,  $a_n^\mu$  and  $\tilde{a}_n^\mu$  are raised to operators satisfying a specific commutation relation. Since  $a_n^\mu, \tilde{a}_n^\mu$  are spacetime vectors and not spinors, the string is said to be bosonic. In such a case,  $D = 26$  for many reasons, one of which being the removal of negative-normed states.

### 3.2 Superstrings

In order to introduce fermions into string theories, one consider superstrings, i.e., strings that exhibit supersymmetry in  $D = 10$  dimensions. There are two equivalent ways to introduce supersymmetry in string theories known as the Green-Schwarz (GS) formalism or the Ramond-Neveu-Schwarz (RNS) formalism. We will focus on the RNS point of view, which starts from a globally supersymmetric *world-sheet* action.

In order to find such action, massless world-sheet fermions  $\psi^\mu$  are added to the Polyakov action through a Dirac term:

$$S = -\frac{T}{2} \int d^2\sigma \left( \partial_a X^\mu \partial^a X_\mu + \bar{\psi}^\mu \gamma^a \partial_a \psi_\mu \right) \quad (3.15)$$

The worldsheet metric  $h^{ab}$  is fixed to the diagonal matrix  $\eta^{ab} \equiv \text{Diag}(-1, 1)$ .  $\gamma^a$  are the two-dimensional Dirac matrices satisfying  $\{\gamma^a, \gamma^b\} = 2\eta^{ab}$  and the components of

$\psi^\mu$  are Grassmann numbers. If  $\beta$  is a Majorana Grassmann-valued spinor, the above action is invariant (up to a total derivative term) under the following transformations:

$$\delta X^\mu = \bar{\beta}\psi^\mu \quad (3.16)$$

$$\delta\psi^\mu = \gamma^a\partial_a X^\mu\beta \quad (3.17)$$

This invariance sets the ground for supersymmetry. Indeed, one rewrites the action enhanced with fermions as a manifestly supersymmetric action which involves a superfield  $Y^\mu(\sigma^a, \theta)$  and a supercovariant derivative  $D_I$  (where I is a supersymmetric index).

$$S_{SUSY} = T \int d^2\sigma d\theta d\bar{\theta} \bar{D}Y^\mu D Y_\mu \quad (3.18)$$

$$Y^\mu = X^\mu + \bar{\theta}\psi^\mu + \frac{1}{2}B^\mu(\sigma^a) \quad (3.19)$$

$$D_I = \frac{\partial}{\partial\bar{\theta}^I} + (\gamma^a\theta)_I\partial_a \quad (3.20)$$

$$\int d\theta d\bar{\theta} \bar{\theta}\theta = -1 \quad (3.21)$$

The EOM of the fermionic fields are given by the conservation of the supercurrents.

In light-cone coordinates, these currents are:

$$J_+ = \psi_+^\mu\partial_+ X_\mu, \quad J_- = \psi_-^\mu\partial_- X_\mu, \quad (3.22)$$

$$\text{Conservation} \Rightarrow \partial_- \psi_+^\mu = 0, \quad \partial_+ \psi_-^\mu = 0 \quad (3.23)$$

As one varies the action (3.15) with respect to the fermionic fields, one must impose certain conditions on them in order to cancel the boundary term. The conditions are different for open and closed strings.

## 1. Open Strings.

One must impose  $\psi_+^\mu|_{\sigma=0,\pi} = \pm \psi_-^\mu|_{\sigma=0,\pi}$ . At one end of the string (say  $\sigma = 0$ ), one can choose the positive sign as a convention, but the sign at the other end leads to different mode expansions.

### (a) Ramond (R) Condition

$$\psi_+^\mu|_{\sigma=\pi} = \psi_-^\mu|_{\sigma=\pi} \quad (3.24)$$

$$\Rightarrow \psi_+^\mu = \frac{1}{\sqrt{2}} \sum_{n \in \mathbb{Z}} d_n^\mu e^{-in\sigma^+} \quad (3.25)$$

$$\psi_-^\mu = \frac{1}{\sqrt{2}} \sum_{n \in \mathbb{Z}} d_n^\mu e^{-in\sigma^-} \quad (3.26)$$

### (b) Neveu-Schwarz (NS) Condition

$$\psi_+^\mu|_{\sigma=\pi} = -\psi_-^\mu|_{\sigma=\pi} \quad (3.27)$$

$$\Rightarrow \psi_+^\mu = \frac{1}{\sqrt{2}} \sum_{n \in \mathbb{Z} + \frac{1}{2}} b_n^\mu e^{-in\sigma^+} \quad (3.28)$$

$$\psi_-^\mu = \frac{1}{\sqrt{2}} \sum_{n \in \mathbb{Z} + \frac{1}{2}} b_n^\mu e^{-in\sigma^-} \quad (3.29)$$

## 2. Closed Strings.

One must impose the anti/periodicity condition  $\psi_a^\mu(\sigma) = \pm \psi_a^\mu(\sigma + \pi)$  for left and right movers. Again, the choice of the sign leads to different mode expansions.

(a) Ramond (R) Condition

$$\psi_{\pm}^{\mu}(\sigma) = \psi_{\pm}^{\mu}(\sigma + \pi) \quad (3.30)$$

$$\Rightarrow \psi_{+}^{\mu} = \frac{1}{\sqrt{2}} \sum_{n \in \mathbb{Z}} \tilde{d}_n^{\mu} e^{-2in\sigma^{+}} \quad (3.31)$$

$$\psi_{-}^{\mu} = \frac{1}{\sqrt{2}} \sum_{n \in \mathbb{Z}} d_n^{\mu} e^{-2in\sigma^{-}} \quad (3.32)$$

(b) Neveu-Schwarz (NS) Condition

$$\psi_{\pm}^{\mu}(\sigma) = -\psi_{\pm}^{\mu}(\sigma + \pi) \quad (3.33)$$

$$\Rightarrow \psi_{+}^{\mu} = \frac{1}{\sqrt{2}} \sum_{n \in \mathbb{Z} + \frac{1}{2}} \tilde{b}_n^{\mu} e^{-2in\sigma^{+}} \quad (3.34)$$

$$\psi_{-}^{\mu} = \frac{1}{\sqrt{2}} \sum_{n \in \mathbb{Z} + \frac{1}{2}} b_n^{\mu} e^{-2in\sigma^{-}} \quad (3.35)$$

### 3.3 Type II Superstring Theories

Among the equivalent formulations of superstring theories, we choose to present the Type II theories in more details since they are the starting points of the QCD models relevant to this research. Type II theories are formulated with closed strings. After the bosonic and fermionic fields of the superstring are quantized and the tachyonic modes are removed with the GSO projection, one may choose R or NS boundary conditions for the left and right-moving fields. The ground state of the R sector is a 8-component Majorana-Weyl spinor ( $|\pm\rangle$ ) whose chirality has to be fixed for both left and right-moving fields. If one chooses the same chirality for both R-sector groundstates, one obtains the Type IIB theory. On the other hand, if the chirality is opposite, one has the Type IIA theory.

Table 3–1: Type IIA vs Type IIB.

Sector	IIA	IIB
R-R	$ -\rangle \otimes  +\rangle$	$ +\rangle \otimes  +\rangle$
R-NS	$ -\rangle \otimes b_{1/2}^i 0\rangle_{NS}$	$ +\rangle \otimes b_{1/2}^i 0\rangle_{NS}$
NS-R	$\tilde{b}_{1/2}^i 0\rangle_{NS} \otimes  +\rangle$	$\tilde{b}_{1/2}^i 0\rangle_{NS} \otimes  +\rangle$
NS-NS	$\tilde{b}_{1/2}^i 0\rangle_{NS} \otimes b_{1/2}^i 0\rangle_{NS}$	$\tilde{b}_{1/2}^i 0\rangle_{NS} \otimes b_{1/2}^i 0\rangle_{NS}$

$b_{1/2}^i$  corresponds to the first fermionic creation operator and  $i = 1, \dots, 8$ . Both NS-NS and R-R sector states correspond to spacetime bosons, while R-NS and NS-R lead to spacetime fermions. In both type IIA and IIB, the NS-NS sector contains 64 states that separate into a traceless symmetric two-tensor  $G_{\mu\nu}$  (Metric), an anti-symmetric two-tensor  $B_{\mu\nu}$  (Kalb-Ramond Field) and a scalar  $\Phi$  (Dilaton) in  $D = 10$  dimensions. In Type IIA, the R-R sector contains a one-form  $(C_1)_\mu$  and a three-form  $(C_3)_{\mu\nu\rho}$  gauge field. In Type IIB, the R-R sector has a zero-form  $C_0$ , a two-form  $(C_2)_{\mu\nu}$  and a four-form  $(C_4)_{\mu\nu\rho\sigma}$  gauge field with a self-dual four-form field strength ( $F_5 = \tilde{F}_5$ ).

Consequently, when one considers D-branes (Section 3.4), which couple to RR gauge-fields and their duals, only those whose world-volume are odd-dimensional (resp. even-dimensional) can be included in Type IIA (resp. Type IIB) string theories. In the low-energy limit, the Type II superstring theories are described by the Type II supergravity action [23, 24].

### 3.4 D-Branes

In open string theories, Dp-branes are  $p + 1$  dimensional objects that arise from the Dirichlet boundary conditions imposed on the string endpoints. They become dynamical from the fact that they receive momentum at the Dirichlet string endpoints by momentum conservation. Indeed, as opposed to the Neuman string, the Dirichlet string is not forced to have a vanishing momentum at its endpoints. Once one adds the massless NS-NS fields of closed strings  $(G_{\mu\nu}, B_{\mu\nu}, \Phi)$ , Dp-Branes interact with these fields and change their shape accordingly. In the low-energy limit, an effective action of this interaction is given by the Dirac-Born-Infeld (DBI) action:

$$S_{DBI} = -T_p \int d^{p+1} \sigma e^{-\tilde{\Phi}} \sqrt{-\det(G_{MN} + B_{MN} + 2\pi\alpha' F_{MN})} \quad (3.36)$$

$$T_p = \frac{1}{(2\pi)^2 \alpha'^{\frac{p+1}{2}} g_s} \quad (3.37)$$

where  $M, N = 1, \dots, p + 1$  and tensors with these indices correspond to induced quantities on the Dp-Brane (eg.  $G_{MN} = \partial_M X^\mu \partial_N X^\nu G_{\mu\nu}$ ).  $F_{\mu\nu}$  is the field-strength of the gauge potential  $A_\mu$ ,  $\tilde{\Phi} = \Phi - \Phi_0 \equiv \Phi - \log(g_s)$  and  $T_p$  is the brane tension [25].

D-branes also couple to the massless RR forms  $C_i$  of the closed string via the Wess-Zumino term.

$$S_{WZ} = -\mu_p \int \sum_i C_i \wedge e^{B+2\pi\alpha' F} = -\mu_p \int \sum_{\substack{i,n, \\ i+2n=p+1}} \frac{1}{n!} C_i \wedge (B + 2\pi\alpha' F)^n \quad (3.38)$$

$$\mu_p = \int_{S^{8-p}} *F_{p+2} = g_s T_p \quad (\text{BPS bound}) \quad (3.39)$$

The RR charge  $\mu_p$  of the Dp-branes saturates the BPS bound, which implies that they are BPS states.

Moreover, when one perturbs the DBI action around the flat NS-NS background in the Einstein frame using the gravitational coupling  $\kappa$  as the expansion parameter, one recovers an action with a Yang-Mills term along with a kinetic term for the scalar fields  $\phi^a$ , which determine the transverse coordinates of the Dp-brane.

$$G_{\mu\nu} = \eta_{\mu\nu} + \kappa h_{\mu\nu}(x), \quad B_{\mu\nu} = 0 + \kappa b_{\mu\nu}(x), \quad \tilde{\Phi} = 0 + \kappa \tilde{\phi}(x) \quad (3.40)$$

$$A^\mu \equiv (A^M, \phi^a), \quad X^\mu = (\sigma^M, 2\pi\alpha'\phi^a) \quad (3.41)$$

$$S_{DBI} = -T_p(2\pi\alpha')^2 \int d^{p+1}\sigma \left( \dots + \frac{1}{4}F_{MN}F^{MN} + \frac{1}{2}\partial_M\phi_a\partial^M\phi^a + \dots \right) \quad (3.42)$$

From this action, we can read the Yang-Mills coupling induced on the Dp-brane.

$$g_{YM}^2 = (T_p(2\pi\alpha')^2)^{-1} \quad (3.43)$$

This is a very efficient technique of producing gauge and scalar fields in  $p + 1$  dimension and it is indeed used in holography QCD models [26]. One can even obtain non-abelian  $SU(N)$  Yang-Mills theories by stacking  $N$  number of Dp-branes.

### 3.5 Compactification

A partial requirement of all holographic QCD models is to provide a QCD theory in four dimensions with a Minkowski signature. Therefore, one has to reduce the ten starting dimensions down to four using several techniques, one being choosing the value of  $p$  (eg.  $p = 3$ ) to recover QCD on a Dp-brane. However, fixing the value of  $p$  only is too restrictive and the desired value is sometimes not allowable in certain types of string theories. For example,  $p = 3$  is not allowed in Type IIA theories.

Alternatively, one may also postulate that the local geometry of the embedding spacetime ( $M$ ) separates into the Cartesian product of a Minkowski spacetime  $M_4$  with a six-dimensional *internal manifold*  $\mathcal{M}_6$ .

$$M = M_4 \times \mathcal{M}_6 \tag{3.44}$$

One proceeds with finding a Yang-Mills theory by integrating over the internal manifold coordinates (*compactification*), which leads to an action with the desired number of dimensions.

There are a couple of conditions in string theories that put restrictions on the type of manifold that  $\mathcal{M}_6$  can be. It is often, if not always, a Calabi-Yau manifold whose properties preserve useful symmetries of the string theory such as supersymmetry.

Without delving into too much detail, Calabi-Yau manifolds are n-complex dimensional Kähler manifolds that possess a specific Ricci flat Kähler metric. The existence of a flat metric is guaranteed by Yau's theorem [27]. They are usually compact, one exception being the *conifold*. Since the first Chern class  $c_1$  of Calabi-Yau manifolds vanishes, they possess a nowhere vanishing holomorphic n-form, which can be used to define a volume form.

### 3.6 T-Duality

T-duality is an important duality of string theories that connects seemingly different theories of superstrings. One of these equivalences that concerns us most is the one which links Type IIA to Type IIB string theories.

First of all, in order to perform a T-duality transformation, one must have a compact spacetime dimension of some characteristic scale  $R$ . For example, let us assume that the  $X^9$  coordinate of a string is compactified such that  $X^9 \sim X^9 + 2\pi R w$  where  $w$  is the winding number. In the RNS formalism, the T-duality transformation of the bosonic field  $X^9$  is described by the following formula:

$$X_L^9 \rightarrow X_L^9, \quad X_R^9 \rightarrow -X_R^9 \quad (3.45)$$

and the associated fermionic field must transform similarly in order to preserve the world-sheet supersymmetry.

$$\psi_L^9 \rightarrow \psi_L^9, \quad \psi_R^9 \rightarrow -\psi_R^9 \quad (3.46)$$

Recall that the difference between Type IIA and IIB theories stemmed from the relative chirality between the left and right R-sector ground states (see section 3.3). Looking at eq. (3.46) and remembering that the R-sector ground states are fermions, it is easy to see that T-duality transformations link the Type II theories. The precise statement is that the Type IIA theory compactified on some circular dimension of radius  $R$  is equivalent to the Type IIB theory compactified on the same circular dimension with dual radius  $\tilde{R} = \alpha'/R$ .

We present the T-duality transformations of the massless NS-NS sector [28], which will be used later in our analysis. T-duality is performed along the 9<sup>th</sup> dimension and the tilded objects represent the new quantities.

$$\tilde{G}_{99} = \frac{1}{G_{99}} \tag{3.47}$$

$$\tilde{G}_{\mu\nu} = G_{\mu\nu} + \frac{B_{9\mu}B_{9\nu} - G_{9\mu}G_{9\nu}}{G_{99}}, \quad \mu, \nu \neq 9 \tag{3.48}$$

$$\tilde{B}_{\mu 9} = \frac{G_{9\mu}}{G_{99}} = -\tilde{B}_{9\mu}, \quad \mu \neq 9 \tag{3.49}$$

$$\tilde{B}_{\mu\nu} = B_{\mu\nu} + \frac{G_{9\mu}B_{9\nu} - B_{9\mu}G_{9\nu}}{G_{99}}, \quad \mu, \nu \neq 9 \tag{3.50}$$

$$\tilde{\phi} = \phi - \frac{1}{2}\log(G_{99}) \tag{3.51}$$

The R-R forms are also transformed by T-duality, but we omit to present them here since they are not necessary for our calculations. Formulas for the T-dual R-R forms can be found in [29].

## CHAPTER 4

### Holography

In this chapter, we will portray the heuristic idea of gauge/gravity dualities by presenting the first holographic equivalence conjectured by Maldacena, namely AdS/CFT. We will also give evidence for the validity of the duality and give explanations on how it is useful in the context of QCD.

#### 4.1 Planar vs Non-Planar Diagrams

In a Yang-Mills theory, one can classify arbitrary connected Feynman diagrams into two types, namely planar and non-planar. Non-planar diagrams possess lines that cross over one another and hence cannot be drawn on the plane without forcing lines to touch. On the contrary, such situations must not happen for planar diagrams. Examples of planar and non-planar diagrams are given below.

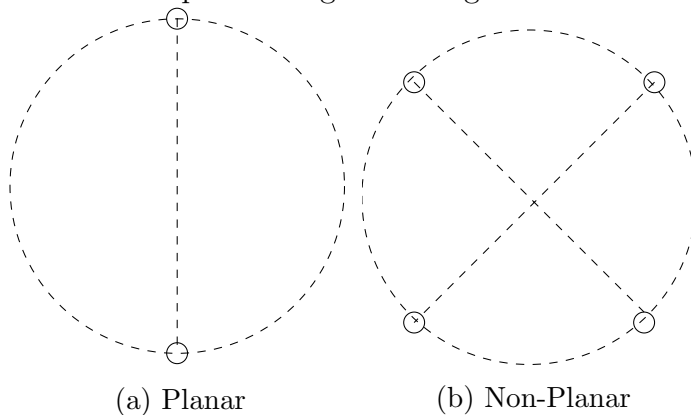


Figure 4-1: Examples of planar and non-planar diagrams.  $\bigcirc$  represents interaction vertices.[1]

The dashed lines in the diagrams correspond to gauge field propagators. Note that the absence of an interaction vertex at the center of diagram 4–1b induces its non-planarity.

## 4.2 Large N Expansion

On a first look, Yang-Mills theories seem to have no dimensionless parameter that one could use to perform a controllable expansion of the Feynman diagrams. Indeed, through dimensional transmutation, the coupling constant  $g_{YM}$  can be transformed into a dimensionful parameter by using the QCD scale  $\Lambda_{QCD}$ . [1] However, if one allows the rank of the gauge group  $SU(N)$  to vary, then,  $N$  would be a dimensionless parameter.

As it was discovered by Gerard 't Hooft [3], planar and non-planar diagrams scale differently with respect to  $N$ . To show the different scaling, 't Hooft introduced a double-line formalism where each gauge field propagator is replaced by two lines making the "flow" of colors more tractable. One could interpret the double lines as a quark-antiquark pair propagating in opposite directions. The double-line version of diagrams 4–1a and 4–1b are drawn as follows where arrows indicate the color flow:

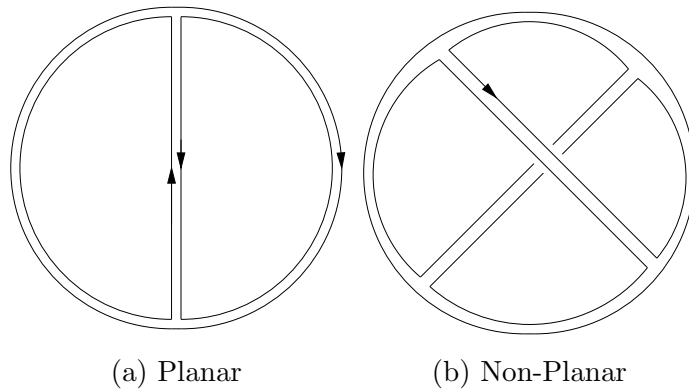


Figure 4–2: Planar and non-planar diagrams in the double-line formalism. [1]

Looking at the QCD Lagrangian (eq. (2.4)) with  $g = g_{YM}$ , we see that gauge field interaction vertices add a factor of  $g_{YM}$  while gauge field propagators add a factor  $\sim 1$ . Also, each inner loop in diagrams drawn in the double-line notation corresponds to a free color index that must be summed, hence it adds a factor of  $N$  to the diagram amplitude. In fact, if one adds an extra inner propagator to an arbitrary diagram and makes sure that this propagator does not cross over existing ones, the amplitude of the diagram changes by a factor of  $(g_{YM})^2 N^1 = g_{YM}^2 N \equiv \lambda$ , where  $\lambda$  is the 't Hooft coupling. Indeed, by adding a propagator free of cross-over points, one adds 2 vertices and 1 loop as explicitly written in the factor calculation. In light of this interesting fact, the 't Hooft coupling becomes a natural expansion parameter for Feynman diagrams.

Now, let us see how our examples of planar and non-planar diagrams scale with respect to  $N$  assuming that  $\lambda$  remains constant. 4-2a has 2 vertices and 2 loops which lead to an amplitude  $A_P \sim g_{YM}^2 N^2 = \lambda N$ . On the other hand, the non-planar diagram 4-2b has 4 vertices and only 1 loop since, imagining a 3D construction of the diagram, one can trace over all the inner lines with a pen without raising the ballpoint. With one less loop, the non-planar diagram amplitude  $A_{NP} \sim g_{YM}^4 N = \lambda^2/N$  is subleading compared to  $A_P$ . This implies that the amplitude of an arbitrary dynamical process will exhibit the following dependence on  $\lambda$  and  $N$ .

$$\mathcal{A} \sim N \left( A(\lambda) + \frac{1}{N^2} B(\lambda) + \frac{1}{N^4} C(\lambda) + \dots \right) \quad (4.1)$$

where  $A(\lambda)$ ,  $B(\lambda)$  and  $C(\lambda)$  are polynomials of  $\lambda$ . The first term in (4.1) corresponds to the contribution of planar diagrams while the other terms are related to non-planar diagrams.[30]

When we take the limit  $N \rightarrow \infty$  and keep  $\lambda$  constant,  $g_{YM}$  must accordingly scale to 0, which means that we probe the low-coupling limit of the Yang-Mills theory. In such case, non-planar diagrams become irrelevant according to (4.1) and the 't Hooft coupling now controls the diagrammatic expansion of the theory.

### 4.3 AdS/CFT from the Low-Energy Spectrum Point of View

AdS/CFT was first conjectured by Juan Maldacena [4] who showed evidence that a  $SU(N)$   $\mathcal{N} = 4$  supersymmetric Yang-Mills theory (a gauge theory) in a Minkowski spacetime was equivalent to a Type IIB superstring theory (a gravity theory) in a spacetime whose geometry is a product of an Anti de-Sitter(AdS) and a spherical geometry, namely  $AdS_5 \times S^5$ . The correspondence was first demonstrated by looking at the low energy excitations of a set of  $N$  coincident D3-branes in Type IIB closed string theory in a ten-dimensional flat target space.  $N$  is fixed and large and the string excitations are smaller than the string energy scale ( $E \ll 1/\sqrt{\alpha'}$ ), which is equivalent to the limit  $\alpha' \rightarrow 0$  with a fixed energy  $E$ . Then, Maldacena analyzed this system in two regimes, namely  $g_s N \gg 1$  and  $g_s N \ll 1$ .

First, let's look at the regime  $g_s N \ll 1$ . In this case, since  $N$  is large, the string coupling is small and the gravitational effects of the D-branes can be neglected. This implies that the open strings attaching on  $N$  coincident D3-branes don't interact to form closed strings but give rise to a  $SU(N)$  Supersymmetric Yang-Mills (SYM) theory in ten-dimensional flat space. Also, by letting  $\alpha' \rightarrow 0$ , the ten-dimensional

Newton constant  $G^{(10)} \sim g_s^2 \alpha'^4$ , which governs the gravitational interaction of strings, becomes very small as well. Consequently, the surrounding type IIB closed strings don't interact with the  $SU(N)$  Yang-Mills fields on the D3-branes. This is known as the decoupling limit where the two decoupled systems are summarized below.

$$\begin{array}{l} \text{N D3-branes in 10D flat space} \\ \text{with Type IIB closed strings} \end{array} \xrightarrow[g_s N \ll 1]{\alpha' \rightarrow 0} \left\{ \begin{array}{l} 1. \text{ Closed strings in flat space} \\ 2. \text{ 4D } SU(N) \text{ SYM theory} \end{array} \right\}$$

In the other regime  $g_s N \gg 1$ , the gravitational effects of the D3 branes cannot be neglected. To realize this fact, one has to look at the gravitational potential of an object of mass  $M$  in ten-dimensional spacetime. Such an object gravitates with the following potential where  $G^{(10)}$  is the ten-dimensional Newton's constant.

$$V(r) = \frac{G^{(10)} M}{r^7} \quad (4.2)$$

In Planck units, the potential is dimensionless, which defines a characteristic scale for gravitational effects, namely  $L \equiv (G^{(10)} M)^{1/7}$ , that is proportional to the Schwarzschild radius. Therefore, when  $L \ll 1$ , the gravitational effects of this mass can be neglected.

If each  $N$  Dp-brane occupies a volume  $V_p$  and is attracting masses gravitationally, then

$$M = N V_p T_p \sim \frac{N V_p}{g_s \alpha'^{\frac{p+1}{2}}} \quad (4.3)$$

and from the point of view of the transverse dimensions, the  $N$  Dp-Branes look like a point mass in  $7 - p$  dimensional space.

$$L^{7-p} = G^{(10-p)} M = \frac{G^{(10)}}{V_p} M \sim g_s N \alpha'^{\left(\frac{7-p}{2}\right)} \quad (4.4)$$

$$\Rightarrow \left( \frac{L}{\sqrt{\alpha'}} \right)^{7-p} \sim g_s N \quad (4.5)$$

We used the fact that  $G^{(10)} \sim g_s^2 \alpha'^4$ . Therefore, when  $g_s N \gg 1$ , the gravitational effects of the  $N$  D3-branes are not negligible.

From the Type IIB supergravity point of view,  $N$  Dp-branes can be understood as BPS solitonic objects possessing RR charges. Their metric solution is given by the following expression:

$$ds^2 = \frac{1}{\sqrt{1 + \frac{L^{7-p}}{r^{7-p}}}} \left( -dt^2 + \sum_{i=1}^p dx^i dx^i \right) + \sqrt{1 + \frac{L^{7-p}}{r^{7-p}}} (dr^2 + r^2 d\Omega^{8-p}) \quad (4.6)$$

$x^i$  corresponds to the transverse coordinates of the D-branes and  $dr^2 + r^2 d\Omega^{8-p}$  is the metric of the orthogonal sphere. The radius  $r$  ranges from 0 to  $\infty$ . However, this supergravity representation is only useful when  $g_s N \gg 1$  because, in that limit, the curvature of the target space in string units ( $\sim \sqrt{\alpha'}/L$ ) is small according to eq. (4.5).

For now, we focus on D3-branes and consider an observer at infinity who measures the energy excitations coming out from this target space. A string excitation has a typical energy  $E = 1/\sqrt{\alpha'}$ . When it is emitted at position  $r$ , the observer at infinity sees this excitation with a redshifted energy  $\sim r/\alpha'$ . Fixing  $r/\alpha'$  while taking

the  $\alpha' \rightarrow 0$  limit corresponds to string excitations that arise from a region close to the origin of the target space. This is commonly called the near-horizon region.

Consequently, if we fix the energy observed at infinity and take  $\alpha' \rightarrow 0$ , the observer sees two types of excitations: 1) finite-energy excitations coming from the near horizon region of the D3-branes and 2) low-energy excitations of closed strings far from the branes. The near-horizon region geometry is found by taking the  $r \ll L$  limit in the D3-brane metric. Note that this is consistent with fixing the energy to  $r/\alpha'$  and taking the  $\alpha' \rightarrow 0$  limit, since  $r \sim \alpha'$  and  $L \sim \sqrt{\alpha'}$  from eq. (4.5). Hence, we obtain the following geometry:

$$ds^2 = \underbrace{\frac{r^2}{L^2} \left( -dt^2 + \sum_{i=1}^3 dx^i dx^i \right)}_{AdS_5} + \frac{L^2}{r^2} dr^2 + \overbrace{L^2 d\Omega^5}^{S^5} \quad (4.7)$$

In other words, the D3-branes have morphed the ten-dimensional Minkowski spacetime at infinity into an  $AdS_5 \times S^5$  geometry near the horizon  $r = 0$ . This geometry possesses an infinite throat with constant circumference surrounded by 5-spheres of radius  $L$ , which is also the radius of curvature of the AdS space. Moreover, the low-energy excitations far from the D3-branes don't interact with the redshifted excitations because their wavelength is too big to probe the size of the throat. In summary, we obtain the following picture:

$$\left. \begin{array}{l} \text{N D3-branes in 10D flat space} \\ \text{with Type IIB closed strings} \end{array} \right\} \begin{array}{l} \xrightarrow[g_s N \gg 1]{\alpha' \rightarrow 0} \\ \left. \begin{array}{l} 1. \text{ Closed strings in flat space} \\ 2. \text{ IIB closed strings on } AdS_5 \times S^5 \end{array} \right\} \end{array}$$

Since  $SU(N)$  Super Yang-Mills theory and Type IIB superstring theory on  $AdS_5 \times S^5$  are both well defined for all values of  $\lambda$ , we obtain the conjectured correspondence by matching the decoupled systems of both regimes with one another ( $1 \leftrightarrow 1, 2 \leftrightarrow 2$ ).

#### 4.4 AdS/CFT from the Symmetries and Parameters Point of View

Another evidence of the AdS/CFT correspondence comes from looking at the symmetries of each theory. First of all, from the gauge theory point of view, the Super Yang-Mills theory has 4D conformal symmetry spanned by fifteen generators and a  $SU(4)$  R-symmetry that rotates the scalar and fermionic component fields of the supermultiplets. From the gravity theory point of view, the conformal symmetry generators are realized as generators of the isometry group  $SO(4,2)$  of the  $AdS_5$  space and the R-symmetry group  $SU(4)$  is mapped to the 5-sphere isometry group  $SO(6)$ , its covering group.

Also, one can map the parameters of each side of the correspondence to the parameters of the original superstring theory system, namely  $g_s$  and  $N$ . On the gauge theory side, the parameters are the coupling constant  $g_{YM}$  and  $N$ . Since open strings attached on the stack of  $N$  D3-branes give rise to  $SU(N)$  bosons, we expect that the Yang-Mills coupling will be proportional to the string coupling. The exact relation is found using eq. (3.37), (3.43) and  $p = 3$ .

$$g_{YM}^2 = (T_3(2\pi\alpha')^2)^{-1} = 2\pi g_s \quad (4.8)$$

On the gravity theory side, the parameters are the string coupling  $g_s$  and the characteristic scale of the D3-brane gravitational effects  $L/\sqrt{\alpha'}$ . As our calculations (4.5)

suggested, we can relate this scale to the 't Hooft coupling in the following way:

$$\frac{L}{\sqrt{\alpha'}} = (4\pi g_s N)^{1/4} \propto \lambda^{1/4} \quad (4.9)$$

Therefore, one can map the two parameters in each side of the correspondence to one another.

$$g_{YM} = \sqrt{2\pi g_s}, \quad N = \frac{1}{2\pi g_s} \left( \frac{L}{\sqrt{\alpha'}} \right)^4 \quad (4.10)$$

$$\text{or} \quad g_s = \frac{g_{YM}^2}{2\pi}, \quad \frac{L}{\sqrt{\alpha'}} = (2 g_{YM}^2 N)^{1/4} \quad (4.11)$$

From these equations, one can see that the AdS/CFT correspondence is weak/strong coupling duality. When  $\lambda \ll 1$ , a weakly couple gauge theory of large  $N$  is dual to a strongly coupled gravitational theory. Indeed, in that case, the second equation in (4.11) tells us that the gravitational theory has a small radius of curvature (strongly curved). Similarly, when  $\lambda \gg 1$ , a strongly couple gauge theory is dual to a weakly coupled gravitational theory.

## CHAPTER 5

### The Sakai-Sugimoto Model

The Sakai-Sugimoto model [10] is one of the successful theories of QCD derived from principles of holography. In particular, they manage to make predictions for the mass of vector and scalar mesons, which closely resemble the experimental values. For this reason, we present an overview of the Sakai-Sugimoto model focusing on the techniques used to derive the vector mesonic spectrum, upon which our calculations are based.

#### 5.1 Essence of the Model

The Sakai-Sugimoto model studies the holographic dual of a non-supersymmetric four-dimensional large  $N_c$  QCD theory with massless flavors. The brane construction is achieved in Type IIA string theory and consists of  $N_f$  pairs of D8/ $\overline{\text{D8}}$ -branes probing a background of  $N_c$  D4 flat branes. As it was done in [9], they use the probe approximation  $N_f \ll N_c$  to neglect the back reaction of the D8 flavor branes. The D4 and D8-branes span the four Minkowski coordinates  $x^i, i = 0, \dots, 3$  where the gauge theory arises. The six-dimensional internal manifold is composed of a four-sphere  $S^4$  along with a radial direction  $U$  and a compact cycle  $S^1$  identified with the coordinate  $x^4$  or  $\tau$ . Diagrammatically, we summarize the embedding of the branes as follows.

Table 5–1: Branes content of the Sakai-Sugimoto model. ● identifies the translational directions.

	$x^0$	$x^1$	$x^2$	$x^3$	$x^4$	$x^5$	$x^6$	$x^7$	$x^8$	$x^9$
$N_c$ D4	●	●	●	●	●					
$N_f$ D8/ $\overline{\text{D8}}$	●	●	●	●		●	●	●	●	●

Fermions are given anti-periodic boundary conditions along the  $x^4$  direction, hence supersymmetry is completely broken. The inverse radius of the  $S^1$ , symbolized as  $M_{KK}$ , provides an energy scale for the gauge theory over which Kaluza-Klein modes are excitable. The D8- $\overline{\text{D8}}$  pairs are only separated in the compactified dimension  $\tau$  and merge at some point  $U(\tau_0) = U_0 > U_{KK}$ .  $U_{KK}$  is the position of an horizon where the  $S^1$  radius vanish.

In this system of D4 and D8/ $\overline{\text{D8}}$  branes, three types of open string modes are relevant for constructing dual QCD particles: 4-4, 4-8 and 4- $\overline{8}$  modes. Each pair of integers indicates the type of D-branes on which the fundamental open strings are attached.

#### 1. 4-4 Strings

The fermions arising from 4-4 strings acquire a mass of order  $M_{KK}$  due to the anti-periodic boundary conditions on the  $x^4$  direction. The massless 4-4 string modes correspond to the gauge field on the D4-brane  $A_\mu^{(D4)}$  ( $\mu = 0 \dots 3$ ) and the scalar fields  $A_4^{(D4)}$ ,  $\phi^i$  ( $i = 5 \dots 9$ ). In the low-energy physics, these modes are

neglected because they only couple with other massless fields through irrelevant operators.

## 2. 4-8 and 4- $\bar{8}$ Strings

The 4-8 and 4- $\bar{8}$  open string modes give rise to  $N_f$  flavors of massless fermions that belong to the fundamental representation of  $U(N_c)$ . For these reasons, these modes are interpreted as fundamental quarks. The 4- $\bar{8}$  quarks have the opposite chirality of the 4-8 quarks. As explained in [32], the D8- $\bar{D}8$  pairs possess a  $U(N_f) \times \overline{U(N_f)}$  gauge symmetry, which is interpreted as the  $U(N_f)_L \times U(N_f)_R$  chiral symmetry in the corresponding gauge theory.

## 3. 8- $\bar{8}$ Strings

To avoid the tachyonic mode of the 8- $\bar{8}$  string modes, the pair of D8- $\bar{D}8$  are sufficiently separated along the  $x^4$  direction to yield a positive squared tachyonic mass. In particular, the  $x^4$  separation has to satisfy the condition:  $\Delta x^4 > \sqrt{2\pi}l_s$ . Given this condition, the tachyonic mass is indeed positive.

$$m_{\text{tachyon}}^2 = \left( \frac{\Delta x^4}{2\pi\alpha'} \right)^2 - \frac{1}{2\alpha'} \quad (5.1)$$

## 5.2 Successes and Limitations

The Sakai-Sugimoto model owes its popularity to several successes which we enumerate here.

### 1. Chiral symmetry breaking.

In the IR limit, the  $N_f$  D8- $\bar{D}8$  pairs merge at some radius  $U = U_0$  due to the shrinking of the  $x^4$  cycle. The gauge symmetry in the gravity picture is therefore reduced to the diagonal component, namely  $U(N_f) \times \overline{U(N_f)} \rightarrow$

$U(N_f)$ , since the D8 and  $\overline{\text{D8}}$ -branes now coincide. This process successfully provides a holographic understanding of the chiral symmetry breaking.

2. Similarities with the hidden local symmetry approach.

The idea of a hidden local gauge symmetry was first suggested by H. Georgi [33, 34]. In this context, the  $\rho$  mesons arise as the gauge bosons of this spontaneously broken hidden symmetry. Universal relations are derived from an action modified with new terms involving the hidden gauge boson. For example, the Kawarabayashi-Suzuki-Riazuddin-Fayyazudin (KSRF) relation [35, 36] connects the couplings of the pions and vector mesons. Such a relation is almost perfectly obtained in the Sakai-Sugimoto model by approximating the non-abelian DBI action of the D8-branes for  $N_f > 1$ .

3. Skyrmion and massless pion.

Another interesting feature that goes along with the chiral symmetry breaking is the appearance of a pion field in the DBI action of the D8-branes. This field is the Nambu-Goldstone boson of the said broken symmetry. They also discover a Skyrme term in the effective low-energy action of the pion, which emerges as a D4 brane wrapped on the internal  $S^4$  from the gravity point of view.

4. Chiral anomaly and the Wess-Zumino-Witten term.

The Wess-Zumino-Witten term of the chiral QCD Lagrangian is found by looking at the Chern-Simons (CS) term of the D8-brane effective action. It is also shown that the  $U(1)_A$  chiral anomaly comes from the CS-term.

5. Mesonic spectrum masses.

And last but not least, upon inserting a gauge flux on the D8-branes and fluctuating their embedding, vector and scalar mesons are found in the DBI action. Their masses are proportional to the Kaluza-Klein mass by the relation  $m_n^2 = \lambda_n M_{KK}^2$  and the constant of proportionality  $\lambda_n$  is determined numerically (see sec.5.4).

Table 5–2: Masses of vector and scalar mesons in the Sakai-Sugimoto model.

Vector Mesons				Scalar Mesons
n	1	2	3	1
$\lambda_n^{CP}$	0.67 <sup>--</sup>	1.6 <sup>++</sup>	2.9 <sup>--</sup>	3.3 <sup>++</sup>
Identification	$\rho(770)$	$a_1(1260)$	$\rho(1450)$	$a_0(1450)$

The model is however not perfect and some aspects could be improved. Examples of these aspects are:

1. Unwanted Kaluza-Klein Modes.

An inconvenient consequence of the compact  $x^4$  cycle is the appearance of an infinite tower of Kaluza-Klein modes above the  $M_{KK}$  scale, which is unexpected in real QCD. One could argue that this mass scale is high enough so that KK modes could never be excited in the low-energy regime. However, such tower of modes is unavoidable if one wants to excite the mesonic modes, since the mesons mass scale is  $M_{KK}$  (see above table 5–2).

## 2. $SO(5)$ symmetry.

The isometry group of the internal  $S^4$  manifold is  $SO(5)$  and this is translated into an exotic  $SO(5)$  symmetry of the dual gauge theory. However, such a symmetry does not exist in QCD. When analyzing the mesonic spectrum, one has to focus on fields which are singlets under this symmetry ( $\mathbf{1}_{SO(5)}$ ) but there is no evidence that other representations would not appear as well.

## 3. Finite temperature defects.

The original model proposed by Sakai and Sugimoto was constructed at zero temperature. Afterwards, people generalized their model for finite temperature and analyzed the realization of the chiral symmetry restoration in the gravity dual, which is expected to happen at high temperature [37]. By increasing the temperature, one would also recognize the confinement/deconfinement phase transition as a Scherk-Schwarz transition in the gravity picture, in which the background of solitonic D4-branes (low temp.) is interchanged with black D4-branes (high temp.). However, it was discovered later that this interpretation of the confinement/deconfinement transition is erroneous since the order parameter of the  $Z_N$  center symmetry has the wrong value in the black brane phase. This was resolved in [38] where it was shown that the confinement/deconfinement transition should be interpreted as a Gregory-Laflamme transition [39].

### 5.3 D8-brane Stability in the D4 Background

Assuming  $N_f \ll N_c$ , we consider a background of  $N_c$  D4-branes probed by  $N_f$  D8-branes, which yields a dual Yang-Mills theory at low-energy scales. For the sake

of clarity, we will focus on the case  $N_f = 1$ . First, the supergravity solution of the D4 background is expressed by a metric and a four-form flux  $F_4 \equiv dC_3$ .

$$ds^2 = \left(\frac{U}{R}\right)^{3/2} (\eta_{\mu\nu} dx^\mu dx^\nu + f(U) d\tau^2) + \left(\frac{R}{U}\right)^{3/2} \left(\frac{dU^2}{f(U)} + U^2 d\Omega_4^2\right) \quad (5.2)$$

$$e^{-\phi} = \frac{1}{g_s} \left(\frac{R}{U}\right)^{3/4}, \quad F_4 = \frac{2\pi N_c}{V_4} \epsilon_4, \quad f(U) = 1 - \frac{U_{KK}^3}{U^3} \quad (5.3)$$

$d\Omega_4^2$ ,  $\epsilon_4$  and  $V_4 = 8\pi^2/3$  refer to the line element, the volume form and the volume of a unit-radius  $S^4$ , respectively.  $R = \sqrt[3]{\pi g_s N_c l_s^3}$  and  $U_{KK}$  are constants. The Kaluza-Klein mass  $M_{KK}$  is related to  $U_{KK}$  as follows:  $M_{KK} = \frac{3}{2} \frac{U_{KK}^{1/2}}{R^{3/2}}$ . The following relations are also useful to translate the supergravity solution to the dual four-dimensional Yang-Mills theory.

$$R^3 = \frac{1}{2} \frac{g_{YM}^2 N_c l_s^2}{M_{KK}}, \quad U_{KK} = \frac{2}{9} g_{YM}^2 N_c M_{KK} l_s^2, \quad g_s = \frac{1}{2\pi} \frac{g_{YM}^2}{M_{KK} l_s} \quad (5.4)$$

Note that the supergravity solution is valid for  $1 \ll g_{YM}^2 N_c \ll \frac{1}{g_{YM}^4}$ .

The D8-branes are embedded in the D4 background by letting the radial coordinate be a function of the compact dimension ( $U = U(\tau)$ ), which results in the following D8-brane metric:

$$ds^2 = \left(\frac{U}{R}\right)^{3/2} \eta_{\mu\nu} dx^\mu dx^\nu + \left( \left(\frac{U}{R}\right)^{3/2} f(U) + \left(\frac{R}{U}\right)^{3/2} \frac{U'^2}{f(U)} \right) d\tau^2 + \left(\frac{R}{U}\right)^{3/2} U^2 d\Omega_4^2 \quad (5.5)$$

The corresponding DBI action leads to an energy-conservation type of law which allows to solve  $U(\tau)$  by quadrature using the initial conditions  $U(0) = U_0$  and  $U'(0) =$

0.

$$S_{D8} \propto \int d^4x d\tau \epsilon_4 e^{-\phi} \sqrt{-\det(g_{D8})} \propto \int d^4x d\tau \epsilon_4 U^4 \sqrt{f(U) + \left(\frac{R}{U}\right)^3 \frac{U'^2}{f(U)}} \quad (5.6)$$

$$\Rightarrow \tau(U) = U_0^4 f(U_0)^{1/2} \int_{U_0}^U \frac{du}{\left(\frac{u}{R}\right)^{3/2} f(u) \sqrt{u^8 f(u) - U_0^8 f(U_0)}} \quad (5.7)$$

Using the above solution, one can find the asymptotic behavior of  $\tau(U)$ , namely  $\tau(\infty)|_{U_0=U_{KK}} = \frac{\delta\tau}{4}$ . In other words, when the merging point  $U_0$  of the D8 and  $\overline{D8}$  branes is at the horizon ( $U_{KK}$ ), their asymptotic position is antipodal in the  $S^1$  geometry ( $\tau_{D8, \overline{D8}} = \pm \frac{\delta\tau}{4}$ ). In fact, Sakai and Sugimoto state that the  $\tau_{D8, \overline{D8}} = \pm \frac{\delta\tau}{4}$  solution is valid for all finite radius  $U$ , which we verified with a numerical approximation of the integral.

Focusing on the case  $U_0 = U_{KK}$ , the D8-brane metric can be cast into two additional forms by transforming the coordinates of the  $(U, \tau)$  plane.

$$y = r \cos(\theta), \quad z = r \sin(\theta) \quad (5.8)$$

$$U^3 = U_{KK}^3 + U_{KK} r^2, \quad \theta \equiv \frac{2\pi}{\delta\tau} = \frac{3U_{KK}^{1/2}}{2R^{3/2}} \tau \quad (5.9)$$

The resulting metrics are:

$$\begin{aligned} ds_{(U,\tau)}^2 &= \left(\frac{U}{R}\right)^{3/2} f(U) d\tau^2 + \left(\frac{R}{U}\right)^{3/2} \frac{dU^2}{f(U)} \\ &= \frac{4}{9} \left(\frac{R}{U}\right)^{3/2} \left(\frac{U_{KK}}{U} dr^2 + r^2 d\theta^2\right) \end{aligned} \quad (5.10)$$

$$= \frac{4}{9} \left(\frac{R}{U}\right)^{3/2} ((1 - h(r)z^2)dz^2 + (1 - h(r)y^2)dy^2 - 2h(r)zydzdy) \quad (5.11)$$

$$h(r) \equiv \frac{1}{r^2} \left(1 - \frac{U_{KK}}{U(r)}\right) \quad (5.12)$$

The  $\tau = \frac{\delta\tau}{4}$  solution translates to  $\theta = \frac{\pi}{2}$  or  $y = 0$ . To check the stability of this configuration, small fluctuations of the embedding coordinate  $y = y(x^0, x^1, x^2, x^3, z)$  are considered near  $y = 0$ . Including terms with at most two powers of the field  $y(x^0, x^1, x^2, x^3, z)$ , the resulting action is given by:

$$S_{D8} \simeq -\tilde{T} \int d^4x dz \left[ U_z^2 + \frac{2R^3}{9U_z} \eta^{\mu\nu} \partial_\mu y \partial_\nu y + y^2 + \frac{U_z^3}{2U_{\text{KK}}} \dot{y}^2 \right] \quad (5.13)$$

$$\tilde{T} \equiv \frac{2}{3} R^{3/2} U_{\text{KK}}^{1/2} T V_4 g_s^{-1}, \quad T = 1/((2\pi)^8 l_s^9), \quad \dot{y} \equiv \partial_z y \quad (5.14)$$

$$U_z(z) \equiv (U_{\text{KK}}^3 + U_{\text{KK}} z^2)^{1/3} \quad (5.15)$$

Since all coefficients in front of the  $y$  terms in eq. (5.13) are positive, the associated energy is also positive. Hence, the D8-brane embedding is stable.

#### 5.4 Masses of Vector Mesons

The gauge field  $A_M$  on the D8-brane has nine components:  $A_\mu$  ( $\mu = 0, 1, 2, 3$ ),  $A_z$  and  $A_\alpha$  ( $\alpha = 5, 6, 7, 8$ ). Focusing on  $SO(5)$  singlet states and assuming that the components don't depend on the coordinates of the  $S^4$  geometry, the non-zero components are  $A_\mu(x^\mu, z)$  and  $A_z(x^\mu, z)$ . Once the  $z$  dimension is integrated out, vector and scalar mesons arise from  $A_\mu(x^\mu, z)$  and  $A_z(x^\mu, z)$  respectively. The DBI action takes a simple form once we make the assumption that the gauge field components are independent of the  $S^4$  geometry:

$$\begin{aligned} S_{D8} &= -T \int d^9x e^{-\phi} \sqrt{-\det(g_{MN} + 2\pi\alpha' F_{MN})} + S_{CS} \\ &= -\tilde{T} (2\pi\alpha')^2 \int d^4x dz \left[ \frac{R^3}{4U_z} \eta^{\mu\nu} \eta^{\rho\sigma} F_{\mu\rho} F_{\nu\sigma} + \frac{9}{8} \frac{U_z^3}{U_{\text{KK}}} \eta^{\mu\nu} F_{\mu z} F_{\nu z} \right] + \mathcal{O}(F^3) \end{aligned} \quad (5.16)$$

Separating the  $x^\mu$  and  $z$  variables using complete sets of functions  $\{\psi_n(z)\}, \{\phi_n(z)\}$  that satisfy a suitable orthonormal condition and an eigenvalue equation, the gauge field components are expanded as follows:

$$A_\mu(x^\mu, z) = \sum_n B_\mu^{(n)}(x^\mu)\psi_n(z) \quad (5.17)$$

$$A_z(x^\mu, z) = \sum_n \varphi^{(n)}(x^\mu)\phi_n(z) \quad (5.18)$$

The orthonormal condition (5.20) and eigenvalue equation (5.19) are determined by demanding that the DBI action terms reduce to the typical mesons terms once the  $z$  integral is performed. The conditions are the following:

$$-K^{1/3} \partial_Z (K \partial_Z \psi_n) = \lambda_n \psi_n \quad (n \geq 1) \quad (5.19)$$

$$\tilde{T}(2\pi\alpha')^2 R^3 \int dZ K^{-1/3} \psi_n \psi_m = \delta_{nm} \quad (5.20)$$

$$Z \equiv \frac{z}{U_{\text{KK}}}, \quad K = K(Z) \equiv 1 + Z^2 = \left( \frac{U_z}{U_{\text{KK}}} \right)^3 \quad (5.21)$$

$$(\phi_m, \phi_n) \equiv \frac{9}{4} \tilde{T}(2\pi\alpha')^2 U_{\text{KK}}^3 \int dZ K \phi_m \phi_n = \delta_{mn} \quad (5.22)$$

From eq. (5.19) and (5.20), one can derive the following condition which fixes the coefficient of the  $B_\mu^{(n)}(x^\mu)$  mass term.

$$\tilde{T}(2\pi\alpha')^2 R^3 \int dZ K \partial_Z \psi_m \partial_Z \psi_n = \lambda_n \delta_{nm} \quad (5.23)$$

To satisfy the  $\phi_n$  condition, one can choose  $\phi_n = m_n^{-1} \dot{\psi}_n$  for  $n \geq 1$  and  $\phi_0 = C/K$  where  $C$  is a suitable normalization constant. With such complete sets, one recovers the typical meson terms of QCD after a suitable gauge transformation that simplifies

the field strength  $F_{\mu z}$  associated to  $A_z$  and  $A_\mu$ .

$$S_{D8} = - \int d^4x \left[ \frac{1}{2} \partial_\mu \varphi^{(0)} \partial^\mu \varphi^{(0)} + \sum_{n \geq 1} \left( \frac{1}{4} F_{\mu\nu}^{(n)} F^{\mu\nu(n)} + \frac{1}{2} m_n^2 B_\mu^{(n)} B^{\mu(n)} \right) \right]. \quad (5.24)$$

$F_{\mu\nu}^{(n)}$  and  $m_n^2 \equiv \lambda_n M_{\text{KK}}^2$  are respectively the four-dimensional field strength and the mass associated to  $B_\mu^{(n)}$ . With this reduced action, it is natural to interpret  $\varphi^{(0)}$  as the pion field and  $B^{\mu(n)}$  as vector mesons.  $\varphi^{(0)}$  turns out to be a pseudo-scalar.

The masses of the vector mesons arising from the D8-brane gauge field are found by studying the eigenvalue equation (5.19). In the large  $z$  limit, we deduce how  $\psi_n(z)$  should behave by demanding that they satisfy eq. (5.20) and (5.23) simultaneously.

$$\psi_n(z) \sim \mathcal{O}(1) \quad \text{or} \quad \mathcal{O}(z^{-1}) \quad (\text{for } z \rightarrow \infty) \quad (5.25)$$

In order to satisfy the normalization condition, the first behavior must be discarded. Since eq. (5.19) is invariant under  $Z \rightarrow -Z$ , we can assume that  $\psi_n$  are either odd or even functions. Proceeding through various algebraic manipulations and using a shooting method, Sakai and Sugimoto managed to find numerical estimates of  $\lambda_n$ . Each  $B^{\mu(n)}$  mode is identified with a well known (axial) vector meson by analyzing its behavior under parity (P) and charge conjugation (C). Borrowing notation from nuclear physics, the eigenvalues are symbolized as  $\lambda_n^{CP}$  where C,P refers to the eigenvalue of the associated mode under the parity and charge conjugation operator, respectively.

The lightest mode ( $\lambda_1$ ) is a vector meson with  $C = -1$  and is interpreted as the  $\rho(770)$  meson. The second lightest mode is an axial-vector with  $C = +1$

interpreted as the  $a_1(1260)$  meson. The third mode is identified with  $\rho(1450)$ , having  $C = P = -1$ .

## 5.5 Masses of Scalar Mesons

A similar analysis has been done for (pseudo) scalar mesons. However, the scalar mesons were found upon fluctuations of the  $y = 0$  D8-brane solution. The action for these fluctuations was found in the stability analysis (see eq. 5.13 ).

$$S_{D8, y^2} \simeq -\frac{4}{9} \tilde{T} R^3 \int d^4x dZ \left[ \frac{1}{2} K^{-1/3} (\partial_\mu y)^2 + \frac{M_{\text{KK}}^2}{2} (K (\partial_Z y)^2 + 2y^2) \right]. \quad (5.26)$$

Separating the coordinates of  $y = y(x^\mu, z)$  again using a complete set of functions  $\{\rho_n, n \geq 1\}$ , which satisfy an eigenvalue equation of the same kind as eq. 5.19, one obtain the following equations:

$$y(x^\mu, z) = \sum_{n=1}^{\infty} \mathcal{U}^{(n)}(x^\mu) \rho_n(Z) \quad (\text{Expansion}) \quad (5.27)$$

$$K^{1/3} \left[ -\partial_Z (K \partial_Z \rho_n) + 2\rho_n \right] = \lambda'_n \rho_n \quad (\text{Eigenvalue eq.}) \quad (5.28)$$

$$\frac{4}{9} \tilde{T} R^3 \int dZ K^{-1/3} \rho_n \rho_m = \delta_{nm} \quad (\text{Orthonormal condition}) \quad (5.29)$$

Using the above identities, one can reduce the action to a simple form:

$$S_{D8, y^2} = \frac{1}{2} \int d^4x \sum_n \left[ (\partial_\mu \mathcal{U}^{(n)})^2 + \lambda'_n M_{\text{KK}}^2 (\mathcal{U}^{(n)})^2 \right] \quad (5.30)$$

It is obvious to see from eq. (5.30) that  $\mathcal{U}^{(n)}$  behaves as a scalar meson with mass  $m_n'^2 \equiv \lambda'_n M_{\text{KK}}^2$ . By looking at the Chern-Simons coupling, one can find the  $C, P$

eigenvalues of the  $\mathcal{U}^{(n)}$  modes by remembering that  $y$  is a scalar field on the D8-brane world-volume. After manipulations similar to the case of vector mesons, Sakai-Sugimoto also found numerical estimates for the mass of  $\mathcal{U}^{(n)}$ . The lightest mode is a scalar with  $C = 1$  and is identified with  $a_0(1450)$ <sup>1</sup>.

Since the mesons' masses are all proportional to the Kaluza-Klein scale  $M_{KK}$ , Sakai and Sugimoto evaluate the accuracy of their QCD model by giving predictions<sup>2</sup> for squared-mass ratios, which are compared with the experimental measurements.

Table 5–3: Sakai-Sugimoto's predictions for ratios of mesons' masses

	Identification	Prediction	Experiment
$\frac{\lambda_2}{\lambda_1}$	$m_{a_1(1260)}^2/m_{\rho(770)}^2$	2.32	2.51
$\frac{\lambda_3}{\lambda_1}$	$m_{\rho(1450)}^2 m_{\rho(770)}^2$	4.22	3.56
$\frac{\lambda'_1}{\lambda_1}$	$m_{a_0(1450)}^2 m_{\rho(770)}^2$	4.76	3.61

---

<sup>1</sup> Note that the  $a_0(1450)$  identification is no longer valid since a lower-mass scalar meson with  $CP = ++$  has been found since the original publication of the Sakai-Sugimoto model. This lighter meson is  $a_0(980)$  [16]

<sup>2</sup> We reproduced the spectrum analysis presented by Sakai and Sugimoto in order to rederive the numerical estimates. We found different decimal places compared with the published results.

## CHAPTER 6

### A UV Complete Model of Holographic QCD

In this chapter, we present the holographic QCD model that has been proposed in [11] and further improved in [2, 40]. Throughout this monograph, this model is referenced as the MDGJ model in recognition of the authors. We summarize its general features and successes as a model of QCD. We also briefly explain the gauge theory and gravity pictures and provide detailed information on the aspects relevant to the mesonic spectrum calculations that we perform in the next chapter.

#### 6.1 Main Building Blocks

The first building block is the Klebanov-Strassler model [41]. This model studies the Yang-Mills theory that arises from a stack of  $N$  D3-branes and  $M$  ( $< N$ ) fractional D3-branes at the apex of a conifold in Type IIB superstring theory. The conifold  $\mathcal{M}_C$  is a Calabi-Yau three-fold whose base  $T^{1,1}$  is an Einstein manifold, which possesses the topology of a product of spheres, namely  $S^2 \times S^3$  [42]. Its metric is given by:

$$ds_{\mathcal{M}_C}^2 = dr^2 + r^2 ds_{T^{1,1}}^2 \tag{6.1}$$

$$ds_{T^{1,1}}^2 = \frac{1}{9} \left( d\psi + \sum_{i=1}^2 \cos(\theta_i) d\phi_i \right)^2 + \frac{1}{6} \sum_{i=1}^2 (d\theta_i^2 + \sin(\theta_i)^2 d\phi_i^2) \tag{6.2}$$

$$0 \leq \theta_i \leq \pi, \quad 0 \leq \phi_i \leq 2\pi, \quad 0 \leq \psi \leq 4\pi \tag{6.3}$$

The fractional D3-branes are D5-branes, which are wrapped around vanishing 2-cycles of  $T^{1,1}$  at the apex ( $r = 0$ ). This brane construction results in a  $\mathcal{N} = 1$  Super Yang-Mills theory whose gauge group is  $SU(N) \times SU(N + M)$ . As was shown in [43], supersymmetry is preserved for zero and low temperatures until the deconfinement temperature is attained. Our analysis focuses on the zero temperature model keeping in mind that we can break SUSY by studying the thermal aspects of the theory at a high enough temperature.

When one studies the running of the two gauge couplings  $g_1 \equiv g_{SU(N)}$  and  $g_2 \equiv g_{SU(N+M)}$ , one can show that their beta functions cannot simultaneously vanish [44]. In fact, the difference of the gauge couplings runs logarithmically due to the presence of fractional D3-branes. In this perspective, the Klebanov-Strassler model goes beyond the usual AdS/CFT picture by proposing a gravity dual of a field theory with a non-trivial RG flow, i.e., non-conformal. Another consequence of the presence of fractional D3-branes is the logarithmic warping of the conifold, which leads to naked singularities in the ten-dimensional metric. This problem is resolved by using a *deformed* conifold as the internal manifold, which incidentally corresponds to breaking the chiral symmetry of the SYM theory.

Building on the Klebanov-Strassler model, the MDGJ model adds  $N_f$  D7 branes according to Ouyang's embedding [45] and a black hole, which introduces the notion of temperature in the dual field theory. Then, various finite temperature calculations are performed (see 6.2) and compared to the lattice QCD predictions. Also, the radial direction of the geometry in the gravity theory is carefully engineered such that the

dual Yang-Mills theory is UV complete, i.e., free of UV divergences like Landau poles [40].

## 6.2 Successes

As we mentioned above, the Klebanov-Strassler model succeeds to find a gravity dual of a non-conformal field theory along the principles of holography, hence generalizing the initial AdS/CFT correspondence. Having foundations similar to the Klebanov-Strassler model, the MDGJ model shares this success. However, a complete picture of holographic QCD remains to be established as we are still missing the asymptotic freedom feature of the high-energy regime. One could view the MDGJ model as one more step towards this sought-after picture of QCD. More precisely, the MDGJ model improvements consist of the construction of a gravity dual of a *thermal* gauge theory with a running coupling and fundamental flavors and the ability to achieve the calculations of the following quantities in the gravity picture <sup>1</sup>

1. Mass and drag of the quark.
2. Wake of the quark produced in the Quark-Gluons Plasma (QGP).
3. Shear viscosity of the QGP
4. Viscosity-to-entropy ratio, though violating the  $1/4\pi$  bound.[7]

Moreover, the model was further improved in [2] by curing the divergences of the UV regime (see sec. 6.4).

---

<sup>1</sup> See sec. 2 of [11] for an overview of the calculations.

### 6.3 Gauge Theory Picture

Our discussion of the gauge theory picture will be succinct, since our calculations are mostly concerned with the gravity picture. First of all, the field theory is conformal for high energies (UV), but shows a confinement behavior for low energies (IR). As calculated in [46], the beta functions of the gauge couplings for the IR regime imply a logarithmic running.

$$\frac{d}{d\log(\Lambda/\mu)} \frac{8\pi^2}{g_1^2} \sim 3N + 3M - 2N(1 - \gamma) \quad (6.4)$$

$$\frac{d}{d\log(\Lambda/\mu)} \frac{8\pi^2}{g_2^2} \sim 3N - 2M(1 - \gamma) - 2N(1 - \gamma) \quad (6.5)$$

$\gamma$  is the anomalous dimension of the  $\text{Tr}(A_i B_j)$  operator (see below) and the flavor dependence has been omitted. In the  $M = 0$  case, the theory is conformal, which implies that  $\gamma = -\frac{1}{2} + O(M/N)$ .

In the Klebanov-Strassler model, the matter fields of the gauge theory are contained in two chiral superfields  $A_i, B_i (i = 1, 2)$  that belong to the  $(N + M, \bar{N})$  and  $(\bar{N} + M, N)$  representations of the gauge group respectively. When the theory flows to the IR regime, the gauge group reduces to  $SU(2M) \times SU(M) \sim SU(M)$  [41] by a series of Seiberg dualities, commonly called a "Duality Cascade" [46]. The quarks in the IR are then in bi-fundamental representations of the gauge group, which differ from the fundamental representations. The MDGJ model fixes this issue with the insertion of  $N_f$  D7 flavor branes where the fundamental quarks are now represented by open strings stretching from the D7-Branes down to the horizon of the black hole. The limitation of this method is that one has to calculate the back reaction of the D7 branes on the geometry, which is not known for the Klebanov-Strassler model, in

order to find the exact gravity dual. These back reaction effects have been considered in the MDGJ model as shown in [11].

Moreover, one can foresee the geometry of the conifold in the gravity theory by looking at the classical field theory. First, one gives expectation values to the  $A_i$  and  $B_i$  gauge fields:

$$\langle A_i \rangle = \text{Diag}(a_i^{(1)}, a_i^{(2)}, \dots, a_i^{(M)}) \quad (6.6)$$

$$\langle B_i \rangle = \text{Diag}(b_i^{(1)}, b_i^{(2)}, \dots, b_i^{(M)}) \quad (6.7)$$

the F-terms equations of the supersymmetric action are automatically satisfied while the D-terms equations and gauge invariance condition imply that:

$$\text{Det}(c^{(k)}) = c_{11}^{(k)} c_{22}^{(k)} - c_{21}^{(k)} c_{12}^{(k)} = 0, \quad k = 1, \dots, M \quad (6.8)$$

$$c_{ij}^{(k)} = a_i^{(k)} b_j^{(k)} \quad (6.9)$$

Eq. (6.8) is one of the defining equations of the conifold where  $c_{ij}^{(k)}$ , for a fixed  $k$ , play the role of four embedding complex coordinates [42]. The index  $(k)$  numbers the  $M$  D3-branes and  $c_{ij}^{(k)}$  correspond to their position on the conifold.

## 6.4 Gravity Picture

Table 6–1: Brane content of the MDGJ model.

	t	x	y	z	r	$\psi$	$\theta_1$	$\phi_1$	$\theta_2$	$\phi_2$
$N$ D3	●	●	●	●						
$M$ D5	●	●	●	●			●	●		
$N_f$ D7/ $\overline{\text{D7}}$	●	●	●	●	●	●			●	●

We start by describing the brane content of the MDGJ model presented in table 6–1. The D7-branes are embedded via Ouyang’s instruction, which states that the D7-branes are the submanifold defined by the following equation:

$$r^{3/2} e^{i(\psi - \phi_1 - \phi_2)} \sin\left(\frac{\theta_1}{2}\right) \sin\left(\frac{\theta_2}{2}\right) = \mu \quad (6.10)$$

$\mu$  is a parameter of the supersymmetric description and can be set to 0 since supersymmetry has to be broken anyway. There are then two possibilities to satisfy the embedding equation:  $\theta_1 = 0, \phi_1 = 0$  (Branch 1) or  $\theta_2 = 0, \phi_2 = 0$  (Branch 2). Following [11], we choose the first option in which the D7-branes are points in the  $(\theta_1, \phi_1)$  plane.

In the gravity picture, the size of the gauge couplings are given in terms of the axio-dilaton  $\tau \equiv C_0 + ie^{-\phi}$  and the NS-NS two-form  $B_2$ .

$$\frac{8\pi^2}{g_1^2} + \frac{8\pi^2}{g_2^2} = 2\pi \text{Im}(\tau) \quad (6.11)$$

$$\frac{8\pi^2}{g_1^2} - \frac{8\pi^2}{g_2^2} = \text{Im}(\tau) \left( \frac{1}{\pi\alpha'} \int_{S^2} B_2 - 2\pi \right) \pmod{2\pi} \quad (6.12)$$

The integral of  $B_2$  is performed on the  $S^2$  of the conifold. In order to obtain a logarithmic running of the coupling in the IR regime (small  $r$ ), it is therefore crucial to have a non-vanishing  $B_2$ . Also, in the far UV regime (large  $r$ ), the gauge theory is conformal, which means that  $H_3 = dB_2$  must vanish (which implies that  $\int_{S^2} B_2$  vanishes by Stokes’ theorem) and the dilaton must be constant ( $e^\phi = g_s$ ). Since the  $H_3$  flux is expected to be a continuous function of  $r$ , it cannot abruptly vanish at a specific  $r$  value.

To have both an IR confinement and a UV conformality, the MDGJ model proposes to partition the radial direction into three regions (see 6–1) with a different brane structure for each. Indeed, it turns out that the behavior of the  $H_3$  flux and warp factor  $h(r)$  can be controlled by the D7-branes.

The first region ranges from the black hole horizon to some radius  $r_{min}$  ( $r_h \leq r \leq r_{min}$ ) and contains  $N_f$  coincident D7-branes. The presence of the D7-branes induces a logarithmic behavior in the warp factor and the three-form flux, which guarantees confinement.

The third region ( $r_0 \leq r < \infty$ ) contains a UV cap that cures the UV divergences of the dual gauge theory and a set of D7-branes *distributed* along the conifold coordinates such that  $N_f = N_f(r, \theta_2, \phi_2)$ . The F-theory constraint [47] on the number of D7-branes is imposed as follows:

$$N_f(r)|_{r>\tilde{r}} = 24 \quad (\tilde{r} > r_0) \quad (6.13)$$

$$N_f(r) = \int_{S^2} N_f(r, \theta_2, \phi_2) d(\cos(\theta_2)) d\phi_2 \quad (6.14)$$

As explained in [2], the fact that  $N_f$  is delocalized allows the possibility to restore the  $1/r^4$  behavior of the warp factor, which means that the asymptotic  $r$  regime would be AdS with vanishing three-form fluxes. Consequently, the dual field theory would be conformal. The price to pay to have delocalized D7-branes is that one must add anti-D5 branes near  $r = r_0$  such that  $h(r)$  still satisfies the background supergravity equations of motion.

The second region ( $r_{min} \leq r \leq r_0$ ) is meant to be an interpolating region between the first and third regions. In this middle range, the  $H_3$  flux decays gradually until it

vanishes completely at  $r = r_0$ , which preserves its continuity. A picture of the three regions is given below where the D7-brane distribution of the third region is shown.

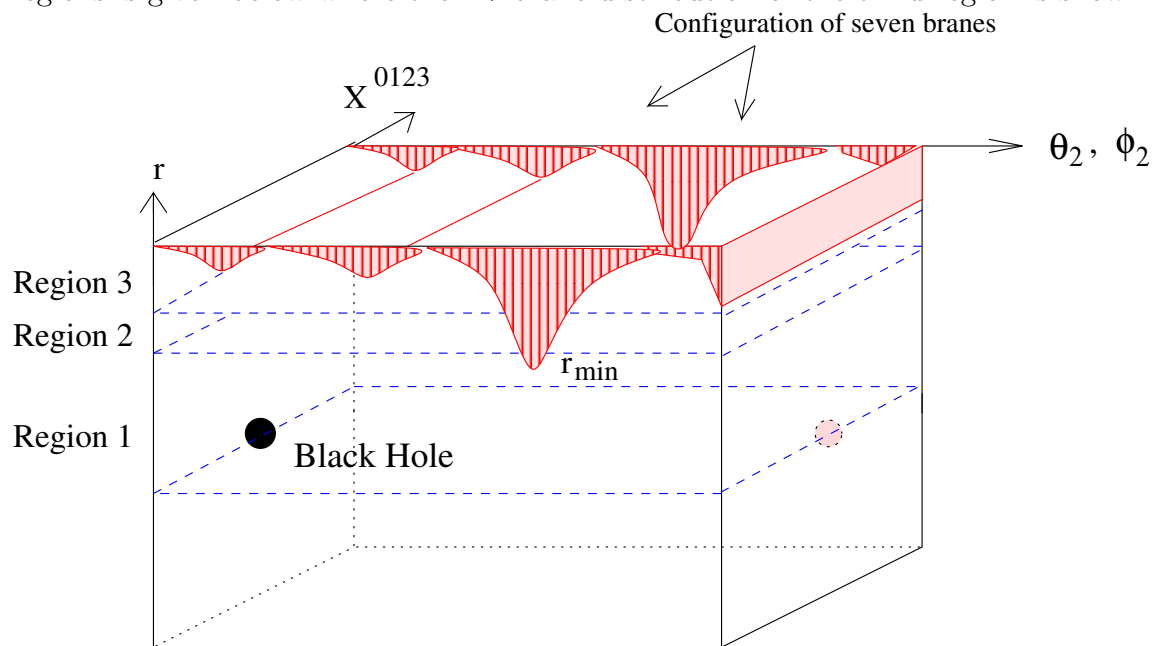


Figure 6-1: D7-brane configuration in the three radial regions. [2]

For the sake of our calculations, we are only concerned with fields in the first region.

Here are the expressions of the relevant fields up to  $O(g_s N_f, g_s M^2/N, g_s^2 M N_f)$  terms.

$$ds^2 = \frac{1}{\sqrt{h}} (-g dt^2 + dx^2 + dy^2 + dz^2) + \sqrt{h} [g^{-1} dr^2 + r^2 d\mathcal{M}_C^2] \quad (6.15)$$

$$e^{-\phi} = \frac{1}{2g_2} \left[ \frac{1}{r^{\epsilon_a}} - \frac{3\epsilon_a a^2}{2r^2} + \text{constant} \right], \quad \epsilon_a = \frac{3g_s N_f}{4\pi} \quad (6.16)$$

$$g(r) = 1 - \frac{r_h^4}{r^4}, \quad L^4 = \frac{27\pi g_s N}{4} \quad (6.17)$$

$$h(r) = \frac{L^4}{r^4} \left[ 1 + \frac{3g_s M_{\text{eff}}^2}{2\pi N} \log(r) \left\{ 1 + \frac{3g_s N_f^{\text{eff}}}{2\pi} \left( \log(r) + \frac{1}{2} \right) + \frac{g_s N_f^{\text{eff}}}{4\pi} \log \left( \sin \frac{\theta_1}{2} \sin \frac{\theta_2}{2} \right) \right\} \right] \quad (6.18)$$

$$\begin{aligned} B_2 = & \left( b_1(r) \cot \frac{\theta_1}{2} d\theta_1 + b_2(r) \cot \frac{\theta_2}{2} d\theta_2 \right) \wedge (d\psi + \cos(\theta_1) d\phi_1 + \cos(\theta_2) d\phi_2) \\ & + \left[ \frac{3g_s^2 M N_f}{4\pi} (1 + \log(r^2 + 9a^2)) \log \left( \sin \frac{\theta_1}{2} \sin \frac{\theta_2}{2} \right) + b_3(r) \right] \sin \theta_1 d\theta_1 \wedge d\phi_1 \\ & - \left[ \frac{g_s^2 M N_f}{12\pi r^2} (-36a^2 + 9r^2 + 16r^2 \log r + r^2 \log(r^2 + 9a^2)) \log \left( \sin \frac{\theta_1}{2} \sin \frac{\theta_2}{2} \right) \right. \\ & \left. + b_4(r) \right] \sin \theta_2 d\theta_2 \wedge d\phi_2 \end{aligned} \quad (6.19)$$

$$b_1(r) = \frac{g_s^2 M N_f}{24\pi(r^2 + 6a^2)} (18a^2 + (16r^2 - 72a^2) \log r + (r^2 + 9a^2) \log(r^2 + 9a^2)) \quad (6.20)$$

$$b_2(r) = -\frac{3g_s^2 M N_f}{8\pi r^2} (r^2 + 9a^2) \log(r^2 + 9a^2) \quad (6.21)$$

$$\begin{aligned} b_3'(r) = & \frac{3g_s M r}{r^2 + 9a^2} + \frac{g_s^2 M N_f}{8\pi r(r^2 + 9a^2)} \left[ \right. \\ & \left. - 36a^2 - 36a^2 \log a + 34r^2 \log r + (10r^2 + 81a^2) \log(r^2 + 9a^2) \right] \end{aligned} \quad (6.22)$$

$$\begin{aligned} b_4'(r) = & -\frac{3g_s M(r^2 + 6a^2)}{\kappa r^3} - \frac{g_s^2 M N_f}{8\pi \kappa r^3} \left[ \right. \\ & \left. 18a^2 - 36(r^2 + 6a^2) \log a + (34r^2 + 36a^2) \log r + (10r^2 + 63a^2) \log(r^2 + 9a^2) \right] \end{aligned} \quad (6.23)$$

$$\kappa = \frac{r^2 + 9a^2}{r^2 + 6a^2} \quad (6.24)$$

$d\mathcal{M}_C^2$  is given in eq. (6.1),  $a$  is the resolution parameter of the conifold,  $N_f^{\text{eff}}$  and  $M^{\text{eff}}$  are equal to  $N_f$  and  $M$ , respectively, to zeroth order in the approximations.

### 6.5 Resemblance with the Sakai-Sugimoto Model

We now show how the MDGJ model looks similar to the Sakai-Sugimoto model after performing a T-duality transformation along the  $\psi$  coordinate of the conifold, which plays the role of the  $x^4$  coordinate of [10]. From the brane content point of view, the resulting T-dual model is summarized as follows:

Table 6–2: Brane content of the  $T_\psi$ -dual MDGJ model.

	t	x	y	z	r	$\psi$	$\theta_1$	$\phi_1$	$\theta_2$	$\phi_2$
$N$ D4	•	•	•	•		•				
$M$ D6	•	•	•	•		•	•	•		
$N_f$ D6/ $\overline{\text{D6}}$	•	•	•	•	•				•	•
NS5	•	•	•	•	•	•			•	•
NS5'	•	•	•	•	•	•	•	•		

The NS5 and NS5' branes are byproducts of T-dualizing the conifold as was described by [48]. In the spectrum analysis, we focus mainly on strings connecting the  $N$  D4 and  $N_f$  D6 branes and forget about the NS5 branes. Unlike the Sakai-Sugimoto model, the D4 branes only span a part of the whole  $\psi$  cycle, which is

depicted in figure 6–2<sup>2</sup> below. This allows us to control the energy scale associated with the compact  $\psi$  dimension, hence making it blind to the 4-dimensional theory.

In comparing the T-dual model, we will assume a zero temperature and focus on the low-energy (IR) regime. In such case, the  $(\theta_1, \phi_1)$  cycle vanishes, i.e., the D6-branes wrapping this cycle become fractional D4-branes. At the apex of the conifold ( $r = 0$ ), these fractional D4-branes are responsible for the remaining  $SU(M)$  gauge group since the  $N$  D4-branes cascade away. In the IR, the  $N_f$  D6/ $\overline{D6}$  branes and the  $N_f$  D8/ $\overline{D8}$  of the Sakai-Sugimoto model behave similarly. Consequently, we also use the probe approximation, i.e., we neglect their back reactions. The IR picture becomes:

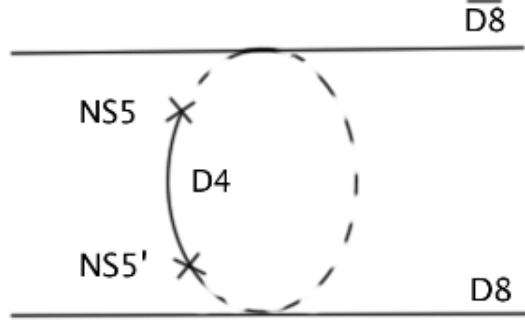
Table 6–3: IR picture of the  $T_\psi$ -dual MDGJ model.

	t	x	y	z	r	$\psi$	$\theta_1$	$\phi_1$	$\theta_2$	$\phi_2$
$N$ D4	●	●	●	●		●				
$M$ Fractional D4	●	●	●	●		●				
$N_f$ D6/ $\overline{D6}$	●	●	●	●	●				●	●
NS5	●	●	●	●	●	●			●	●
NS5'	●	●	●	●	●	●	●	●		

---

<sup>2</sup> Thanks to Long Chen who provided me with this picture.

Figure 6–2: Span of the D4-branes in the  $\psi$  dimension.



The T-dual metric and  $B_2$  form are found using the rules given in sec. 3.6. Using the assumptions  $a \approx 0$ <sup>3</sup>,  $g_s N_f \approx 0$ , we can simplify the expressions given in sec. 6.4.

$$ds^2 = \frac{-dt^2 + dx^2 + dy^2 + dz^2}{\sqrt{h(r)}} + \frac{9L^4}{r^2 \sqrt{h(r)}} d\psi^2 + \sqrt{h(r)} (dr^2 + r^2 d\Sigma^2) \quad (6.25)$$

$$d\Sigma^2 \equiv \frac{1}{6} (d\theta_1^2 + d\theta_2^2 + \sin^2(\theta_1) d\phi_1^2 + \sin^2(\theta_2) d\phi_2^2) \quad (6.26)$$

$$B = 3g_s M \log(r/\mathcal{A}^{2/3}) (\sin(\theta_1) d\theta_1 \wedge d\phi_1 + \sin(\theta_2) d\theta_2 \wedge d\phi_2) + 2L^2 d\psi \wedge (\cos(\theta_1) d\phi_1 + \cos(\theta_2) d\phi_2) \quad (6.27)$$

$$e^{-\phi(r)} = \frac{h(r)^{\frac{1}{4}} r}{6g_s} \quad (6.28)$$

$$h(r) = \frac{27\pi g_s N \left( 1 + \frac{3g_s M_{\text{eff}}^2 \log(r/\mathcal{A}^{2/3})}{2\pi N} \right)}{4r^4} \quad (6.29)$$

We are now ready to perform the mesonic spectrum calculations following the techniques of the Sakai-Sugimoto model.

<sup>3</sup> As explained in [49], the  $a \log(a)$  terms in  $B_2$  don't introduce divergences in the  $a \rightarrow 0$  limit.

## CHAPTER 7

### Mesonic Spectrum Calculations

In this last chapter, we analyze the mesonic spectrum of the T-dual MDGJ model following the methods used by Sakai and Sugimoto in [10]. We calculate the squared-mass ratios of various vector mesons and compare them with the Sakai-Sugimoto predictions and the experimental values taken from the Particle Data Group [16].

#### 7.1 D8-Brane Metric and B-field

In order to simplify the DBI action, we perform the following coordinate transformations similar to what Sakai and Sugimoto did.  $\mathcal{A}^{2/3}$  is the minimal value of  $r$  and is non-zero.

$$Y = \rho \cos(\theta), \quad Z = \rho \sin(\theta) \quad (7.1)$$

$$\rho = \sqrt{Y^2 + Z^2}, \quad \theta = \arctan\left(\frac{Z}{Y}\right) \quad (7.2)$$

$$r = \mathcal{A}^{2/3} e^\rho, \quad \psi = 2\theta \quad (7.3)$$

In the new coordinates, the metric  $G$  and two-form  $B_2$  become:

$$ds_{(r,\psi)}^2 = \frac{9L^4}{r^2\sqrt{h(r)}}d\psi^2 + \sqrt{h(r)}dr^2 \quad (7.4)$$

$$= \frac{\left(e^{\sqrt{Y^2+Z^2}}(Y^2+Z^2)\right)^{-2}}{\mathcal{A}^{4/3}\sqrt{h(r(Y,Z))}} \left(A(Y,Z)(dY^2+dZ^2) + 2B(Y,Z)dYdZ\right)$$

$$A(Y,Z) = \mathcal{A}^{8/3}e^{4\sqrt{Y^2+Z^2}}(Y^2+Z^2)h(r(Y,Z))Y^2 + 36L^4Z^2 \quad (7.5)$$

$$B(Y,Z) = YZ \left(\mathcal{A}^{8/3}e^{4\sqrt{Y^2+Z^2}}(Y^2+Z^2)h(r(Y,Z)) - 36L^4\right) \quad (7.6)$$

$$B_2 = 3g_s M \log(r(Y,Z)/\mathcal{A}^{2/3}) (\sin(\theta_1)d\theta_1 \wedge d\phi_1 + \sin(\theta_2)d\theta_2 \wedge d\phi_2) + \quad (7.7)$$

$$\frac{4L^2}{Y^2+Z^2} (YdZ - ZdY) \wedge (\cos(\theta_1)d\phi_1 + \cos(\theta_2)d\phi_2)$$

## 7.2 D8-Brane Embedding

We proceed by embedding a stack of  $N_f$  D6-branes in this background. We use the first branch of the Ouyang embedding where  $(\theta_1, \phi_1) = (0, 0)$ . Then, we consider the  $\psi$  coordinate as a function of  $r$  ( $\psi(r)$ ) and use the equation of motion for this field to find the behavior of  $\psi(r)$ . Introducing this embedding in the metric and  $B_2$ -field presented above, we obtain the following DBI action:

$$g_{D6MN}dX^M dX^N$$

$$= \frac{-dt^2 + dx^2 + dy^2 + dz^2}{\sqrt{h(r)}} + \left(\frac{9L^4}{r^2\sqrt{h(r)}}\psi'(r)^2 + \sqrt{h(r)}\right) dr^2 + \sqrt{h(r)}r^2 (d\theta_2^2 + \sin(\theta_2)d\phi_2^2) \quad (7.8)$$

$$B_{D6} = 3g_s M \log(r/\mathcal{A}^{2/3}) \sin(\theta_2) d\theta_2 \wedge d\phi_2 + 2L^2\psi'(r)^2 dr \wedge \cos(\theta_2) d\phi_2 \quad (7.9)$$

$$\sqrt{-\det(g_{D6} + B_{D6})} = \sqrt{\frac{L^4 r^2 \psi'(r)^2}{6h(r)^{3/2}} + \sin^2(\theta_2) \left( \frac{(g_s M \log(\frac{r}{A^{2/3}}))^2}{4r^2 h(r)^{5/2}} (81L^4 \psi'(r)^2 + 9h(r)r^2) + \frac{L^4 r^2 \psi'(r)^2}{12h(r)^{3/2}} + \frac{r^4}{36\sqrt{h(r)}} \right)}$$
(7.10)

Setting  $M$  and  $M_{\text{eff}}$  to 0 in the DBI action, we get a simplified expression:

$$S_{D6} = -T \int d^4x dr d\theta_2 e^{-\phi(r)} \sqrt{-\det(g_{D6} + B_{D6})}$$
(7.11)

$$= -T \int d^4x dr d\theta_2 \frac{\pi^{3/4} r^3 \sqrt{2 \sin^2(\theta_2) - 3r^2 (\cos(2\theta_2) - 5) \psi'(r)^2}}{18 \cdot 3^{3/4} \sqrt{N} g_s^{5/4}}$$
(7.12)

The Euler-Lagrange equation is equivalent to the following differential equation:

$$\frac{\pi^{3/4} r^4 (5 - \cos(2\theta_2)) (-6r^2 (\cos(2\theta_2) - 5) \psi'(r)^3 + r \sin^2(\theta_2) \psi''(r) + 5 \sin^2(\theta_2) \psi'(r)^2)}{3 \cdot 3^{3/4} \sqrt{N} g_s^{5/4} (2 \sin^2(\theta_2) + 3r^2 (5 - \cos(2\theta_2)) \psi'(r)^2)^{3/2}} = 0$$
(7.13)

As we can see,  $\psi(r) = \text{constant}$  solves the equation. Coming back to the full DBI action, one can consider  $\delta \equiv \frac{g_s M^2}{N}$  as a small parameter (see section 7.4) and solve the embedding equation order by order in  $\delta$ . Setting  $\psi(r)^{(0)} = \text{constant}$ , the first-order equation becomes:

$$\frac{\left( \left( \frac{\pi}{3} \right)^{3/4} r^4 (5 - \cos(2\theta_2)) \csc(\theta_2) \left( 5\psi^{(1)'}(r) + r\psi^{(1)''}(r) \right) \right)}{6 \left( \sqrt{2} (N g_s^5)^{1/4} \right)} = 0$$
(7.14)

We see that  $\psi(r)^{(1)} = \text{constant}$  is again a solution. In other words,  $\psi(r) = \text{constant}$  solves the Euler-Lagrange equation up to first order in  $\delta$ . Our spectrum analysis does not consider the next orders in  $\delta$ . Consequently, the constant embedding for the  $\psi$  coordinate of the D6-branes is a valid solution. Since the constant value of  $\psi$

is arbitrary, we set the D6-branes and  $\overline{\text{D6}}$ -branes at antipodal positions, respectively. In other words,  $\theta = \frac{\pi}{2}$  for the D6-branes and  $\theta = -\frac{\pi}{2}$  for the  $\overline{\text{D6}}$ -branes. In the  $(Y, Z)$  coordinates, this embedding is equivalent to setting  $Y = 0$ , which considerably simplifies the metric  $g_{D6}$  and NS-NS form  $B_{D6}$ .

$$\begin{aligned} ds^2 &= g_{D6MN} dx^M dx^N \\ &= \frac{-dt^2 + dx^2 + dy^2 + dz^2}{\sqrt{h(r(0, Z))}} + \sqrt{h(r(0, Z))} \mathcal{A}^{4/3} e^{2|Z|} (dZ^2 + d\theta_2^2 + \sin(\theta_2) d\phi_2^2) \end{aligned} \quad (7.15)$$

$$B_{D6} = 3g_s M \log(r(0, Z)/\mathcal{A}^{2/3}) \sin(\theta_2) d\theta_2 \wedge d\phi_2 \quad (7.16)$$

### 7.3 D8-Brane Action with Flux

We first consider the unflavored case ( $N_f = 1$ ) of our brane construction and introduce a gauge flux ( $A_M$ ) along the Minkowski and  $Z$  dimensions.

$$A_M = \begin{cases} A_\mu & \text{when } M = \mu \in \{t, x, y, z\} \\ A_Z & \text{when } M = Z \\ 0 & \text{when } M \in \{\theta_1, \phi_1, \theta_2, \phi_2\} \end{cases} \quad (7.17)$$

$$F_{MN} = \partial_M A_N - \partial_N A_M \quad (7.18)$$

We then look at terms quadratic in  $\alpha'$  in the DBI action where vector mesons arise from the gauge components on the D6-Brane.

$$\begin{aligned}
& \sqrt{-\det(g_{D6} + B_{D6} + 2\pi\alpha'F)} = \\
& \frac{e^{-|Z|} |\sin(\theta_2)|}{6 \mathcal{A}^{2/3} h(r(0, Z))^{3/4}} (81(g_s M Z)^2 + h(r(0, Z)) \mathcal{A}^{8/3} e^{4|Z|})^{1/2} \\
& [\mathcal{A}^{4/3} e^{2|Z|} + \pi^2 \alpha'^2 (2 \eta^{\mu\nu} F_{\mu Z} F_{\nu Z} + \mathcal{A}^{4/3} e^{2|Z|} h(r(0, Z)) \eta^{\mu\nu} \eta^{\rho\sigma} F_{\mu\rho} F_{\nu\sigma}) + O(\alpha'^3)]
\end{aligned} \tag{7.19}$$

$$\begin{aligned}
S_{D6} &= -T \int d^4x dZ d\theta_2 d\phi_2 e^{-\phi(r(0, Z))} \sqrt{-\det(g_{D6} + B_{D6} + 2\pi\alpha'F)} \\
&= -T \int d^4x dZ C(Z) [\mathcal{A}^{4/3} e^{2|Z|} + \pi^2 \alpha'^2 (2 \eta^{\mu\nu} F_{\mu Z} F_{\nu Z} + \mathcal{A}^{4/3} e^{2|Z|} h(r(0, Z)) \eta^{\mu\nu} \eta^{\rho\sigma} F_{\mu\rho} F_{\nu\sigma})]
\end{aligned} \tag{7.20}$$

$$C(Z) \equiv \frac{2\pi e^{-|Z| - \phi(r(0, Z))}}{3 \mathcal{A}^{2/3} h(r(0, Z))^{3/4}} (81(g_s M Z)^2 + h(r(0, Z)) \mathcal{A}^{8/3} e^{4|Z|})^{1/2} \tag{7.21}$$

$$d^4x \equiv dt dx dy dz \tag{7.22}$$

We now expand  $A_\mu$  and  $A_Z$  in eigenmodes using two sets of eigenfunctions  $\{\alpha_n(Z), n \geq 1\}$  and  $\{\beta_n(Z), n \geq 0\}$  whose orthogonality conditions are defined later.

$$A_\mu(x^\mu, Z) = \sum_{n=1}^{\infty} B_\mu^{(n)}(x^\mu) \alpha_n(Z) \quad (7.23)$$

$$A_Z(x^\mu, Z) = \sum_{n=0}^{\infty} \varphi_\mu^{(n)}(x^\mu) \beta_n(Z) \quad (7.24)$$

$$\begin{aligned} \Rightarrow F_{\mu\nu} &= \sum_{n=1}^{\infty} (\partial_\mu B_\nu^{(n)}(x^\mu) - \partial_\nu B_\mu^{(n)}(x^\mu)) \alpha_n(Z) \\ &= \sum_{n=1}^{\infty} F_{\mu\nu}^{(n)} \alpha_n(Z) \end{aligned} \quad (7.25)$$

$$F_{\mu Z} = \partial_\mu \varphi^{(0)}(x^\mu) \beta_0(Z) + \sum_{n=1}^{\infty} (\partial_\mu \varphi^{(n)}(x^\mu) \beta_n(Z) - B_\mu^{(n)}(x^\mu) \dot{\alpha}_n(Z)) \quad (7.26)$$

Focusing on terms proportional to  $\alpha'^2$  and forgetting about  $\beta_0(Z)$  for now, we substitute these expansions in the action.

$$\begin{aligned} S_{\alpha'^2} &= -(T\pi^2 \alpha'^2) \int d^4x dZ C(Z) \sum_{m,n} [\mathcal{A}^{4/3} e^{2|Z|} h(r(0, Z)) F_{\mu\nu}^{(n)} F^{\mu\nu(m)} \alpha_n \alpha_m \\ &\quad + 2 (\partial_\mu \varphi^{(n)} \partial^\mu \varphi^{(m)} \beta_n \beta_m - 2B_\mu^{(m)} \partial^\mu \varphi^{(n)} \dot{\alpha}_m \beta_n + B_\mu^{(m)} B^{\mu(n)} \dot{\alpha}_m \dot{\alpha}_n)] \end{aligned} \quad (7.27)$$

The terms proportional to products of the  $\alpha_n$  eigenfunctions resemble the vector mesons terms of the QCD action.

$$\begin{aligned} S_{B_\mu} &= -(T\pi^2 \alpha'^2) \int d^4x dZ C(Z) \sum_{m,n} [\mathcal{A}^{4/3} e^{2|Z|} h(\mathcal{A}^{2/3} e^{|Z|}) F_{\mu\nu}^{(n)} F^{\mu\nu(m)} \alpha_n \alpha_m \\ &\quad + 2B_\mu^{(m)} B^{\mu(n)} \dot{\alpha}_m \dot{\alpha}_n] \end{aligned} \quad (7.28)$$

In order to recover the typical coefficient of each term, we impose the following orthogonality condition and eigenvalue equation on the  $\alpha_n$  modes.

$$(T\pi^2\alpha'^2) \int dZ C(Z) h(\mathcal{A}^{2/3}e^{|Z|}) \mathcal{A}^{4/3}e^{2|Z|} \alpha_m \alpha_n = \frac{1}{4} \delta_{mn} \quad (7.29)$$

$$-\partial_Z (C(Z) \partial_Z \alpha_n) = h(\mathcal{A}^{2/3}e^{|Z|}) \mathcal{A}^{4/3}e^{2|Z|} C(Z) m_n^2 \alpha_n \quad (7.30)$$

$$\Rightarrow \quad 2(T\pi^2\alpha'^2) \int dZ C(Z) \dot{\alpha}_m \dot{\alpha}_n = \frac{1}{2} m_n^2 \delta_{mn} \quad (7.31)$$

$m_n^2 \equiv \lambda_n M^2$  is the effective squared-mass of each vector meson and  $\lambda_n$  is the eigenvalue of the corresponding mode. The mass scale  $M^2$  is given by  $\frac{\mathcal{A}^{4/3}}{4\pi g_s N}$ .

Regarding the  $\beta_n$  eigenfunctions, we use the same kind of arguments as Sakai and Sugimoto. In order to normalize the kinetic term  $\partial_\mu \varphi^{(n)} \partial^\mu \varphi^{(m)}$  to its canonical form, we impose the following normalization condition for  $\beta_n$ :

$$(T\pi^2\alpha'^2) \int_{-\infty}^{\infty} dZ 2C(Z) \beta_m \beta_n = \frac{1}{2} \delta_{mn} \quad (7.32)$$

It is easily seen that choosing  $\beta_n \equiv \frac{\dot{\alpha}_n}{m_n}$  for  $n \geq 1$  will give us the necessary condition. Also, assuming that we are in a gauge where  $\lim_{Z \rightarrow \pm\infty} A_\mu(Z) = 0$ , we set  $\beta_0 \equiv \frac{K}{C(Z)}$  for some normalization constant  $K$ . The fact that  $A_\mu(Z)$  asymptotically vanishes guarantees orthogonality between  $\beta_0$  and  $\dot{\alpha}_n, \forall n \geq 1$ .

$$2(T\pi^2\alpha'^2) \int dZ C(Z) \beta_0 \dot{\alpha}_n = 2TK \int_{-\infty}^{\infty} dZ \partial_Z \alpha_n \quad (7.33)$$

$$= 0 \quad (7.34)$$

Going back to our expression for  $F_{\mu Z}$ , we have:

$$F_{\mu Z} = \partial_\mu \varphi^{(0)} \beta_0(Z) + \sum_{n=1}^{\infty} (m_n^{-1} \partial_\mu \varphi^{(n)} - B_\mu^{(n)}) \dot{\alpha}_n(Z) \quad (7.35)$$

Absorbing  $m_n^{-1} \partial_\mu \varphi^{(n)}$  into  $B_\mu^{(n)}$  with the gauge transformation:

$$B_\mu^{(n)} \rightarrow B_\mu^{(n)} + m_n^{-1} \partial_\mu \varphi^{(n)} \quad (7.36)$$

we obtain the typical QCD action where  $\varphi^{(0)}(x^\mu)$  is the Nambu-Goldstone boson of the broken chiral symmetry.

$$S_{QCD} = - \int d^4x \left( \frac{1}{2} \partial_\mu \varphi^{(0)} \partial^\mu \varphi^{(0)} + \sum_{n=1}^{\infty} \left[ \frac{1}{4} F_{\mu\nu}^{(n)} F^{\mu\nu(n)} + \frac{1}{2} m_n^2 B_\mu^{(n)} B^{\mu(n)} \right] \right) \quad (7.37)$$

## 7.4 Vector Mesons

We now solve the eigenvalue equation (7.30) by using simple perturbation techniques. We first introduce some notation that will set the problem in the typical perturbation theory definitions. The eigenvalue equation (7.30) can be rewritten as a differential operator  $\mathbf{H}_v$  acting on its eigenfunctions  $\alpha_n$ .

$$(7.30) \rightarrow - \frac{1}{M^2 h(\mathcal{A}^{2/3} e^{|Z|}) \mathcal{A}^{4/3} e^{2|Z|}} \left( \partial_Z^2 + \frac{C'(Z)}{C(Z)} \partial_Z \right) \alpha_n = \lambda_n \alpha_n \quad (7.38)$$

$$\mathbf{H}_v \equiv - \frac{1}{M^2 h(\mathcal{A}^{2/3} e^{|Z|}) \mathcal{A}^{4/3} e^{2|Z|}} \left( \partial_Z^2 + \frac{C'(Z)}{C(Z)} \partial_Z \right) \quad (7.39)$$

$$f(Z) \equiv 4(T\pi^2 \alpha'^2) C(Z) h(\mathcal{A}^{2/3} e^{|Z|}) \mathcal{A}^{4/3} e^{2|Z|} \quad (7.40)$$

$$\langle \alpha_m | \alpha_n \rangle \equiv \int_{-\infty}^{\infty} dZ f(Z) \alpha_m \alpha_n = \delta_{mn} \quad (7.41)$$

We use  $\delta \equiv \frac{g_s M^2}{N}$  as the controlling parameter and expand the eigenfunctions, eigenvalues, differential operator and orthogonality condition as follows <sup>1</sup> :

$$\alpha_n = \alpha_n^{(0)} + \delta \alpha_n^{(1)} + \delta^2 \alpha_n^{(2)} + \dots \quad (7.42)$$

$$\lambda_n = \lambda_n^{(0)} + \delta \lambda_n^{(1)} + \delta^2 \lambda_n^{(2)} + \dots \quad (7.43)$$

$$\mathbf{H}_v = \mathbf{H}_v^{(0)} + \delta \mathbf{H}_v^{(1)} + \delta^2 \mathbf{H}_v^{(2)} + \dots \quad (7.44)$$

$$\langle \cdot | \cdot \rangle = \int_{-\infty}^{\infty} dZ f^{(0)}(Z) + \delta \int_{-\infty}^{\infty} dZ f^{(1)}(Z) + \delta^2 \int_{-\infty}^{\infty} dZ f^{(2)}(Z) + \dots \quad (7.45)$$

$$\equiv \langle \cdot | \cdot \rangle^{(0)} + \delta \langle \cdot | \cdot \rangle^{(1)} + \delta^2 \langle \cdot | \cdot \rangle^{(2)} + \dots \quad (7.46)$$

Using this new notation, the problem is simply stated as:

$$\mathbf{H}_v |\alpha_n\rangle = \lambda_n |\alpha_n\rangle \quad \text{with} \quad \langle \alpha_m | \alpha_n \rangle = \delta_{mn} \quad (7.47)$$

---

<sup>1</sup> We clarify a possible confusion on the  $(n)$  superscript. On  $B_\mu^{(n)}$  and  $\varphi^{(n)}$ ,  $n$  indexes the various fields encountered in the 4-dimensional theory. On  $\alpha_n^{(i)}$ ,  $\lambda_n^{(i)}$ ,  $\mathbf{H}_v^{(i)}$  and  $f^{(i)}$ ,  $i$  refers to the order in the  $\delta$  expansion.

### 7.4.1 Zeroth-Order Eigenvalue

Solving eq. (7.47) order by order in  $\delta$ , we first have<sup>2</sup> :

$$\mathbf{H}_v^{(0)}|\alpha_n^{(0)}\rangle = \lambda_n^{(0)}|\alpha_n^{(0)}\rangle \quad \text{with} \quad \langle\alpha_m^{(0)}|\alpha_n^{(0)}\rangle^{(0)} = \delta_{mn} \quad (7.48)$$

$$\mathbf{H}_v^{(0)} = -e^{2|Z|} (\partial_Z^2 + 2 \text{sign}(Z) \partial_Z) \quad (7.49)$$

$$f^{(0)} = 2T\alpha'^2 \left( \frac{3N^3\pi^{15}}{4g_s} \right)^{1/4} \quad (7.50)$$

As in the Sakai-Sugimoto model, the differential operator is invariant under  $Z \rightarrow -Z$ , which means that  $\alpha_n^{(0)}(Z)$  and  $\alpha_n^{(0)}(-Z)$  solve the same differential equation. Using the uniqueness of the solution to this boundary value problem, we conclude that  $\alpha_n^{(0)}(-Z) \propto \alpha_n^{(0)}(Z)$ . By rescaling the proportionality constant with the normalization condition, two cases are possible.

$$\alpha_n^{(0)}(-Z) = \pm \alpha_n^{(0)}(Z) \quad (7.51)$$

In other words, the solutions are either odd or even in  $Z$ . We remove the upper index (0) to simplify the appearance of the differential equation.

$$\ddot{\alpha}_n(Z) + 2 \text{sign}(Z) \dot{\alpha}_n(Z) + e^{-2|Z|} \lambda_n \alpha_n(Z) = 0 \quad (7.52)$$

Since  $\text{sign}(Z)$  is discontinuous at  $Z = 0$ , we solve the differential equation (7.52) in two regimes, namely  $Z > 0$  and  $Z < 0$ , with which we construct piecewise solutions

---

<sup>2</sup> We assume that the identification  $\text{sign}(Z) = \frac{Z}{|Z|}$  is valid for all values of  $Z$ . This equality is in general incorrect at  $Z = 0$ . But since the point  $Z = 0$  has zero measure, the values of the  $Z$  integrals and the eigenvalues should not change.

for the full equation. The solutions that we obtain for each regime are given in terms of Bessel functions.

$$\alpha_n^{Z>0}(Z) = A_1 e^{-Z} J_1(\sqrt{\lambda_n} e^{-Z}) + A_2 e^{-Z} Y_1(\sqrt{\lambda_n} e^{-Z}) \quad (7.53)$$

$$\alpha_n^{Z<0}(Z) = A_1 e^Z J_1(\sqrt{\lambda_n} e^Z) + A_2 e^Z Y_1(\sqrt{\lambda_n} e^Z) \quad (7.54)$$

$J_1$  is the first Bessel Function of the first kind,  $Y_1$  is the first Bessel function of the second kind and  $A_1, A_2$  are arbitrary coefficients. We set  $A_2 = 0$  since  $e^{\mp Z} Y_1(\sqrt{\lambda_n} e^{\mp|Z|})$  doesn't vanish as  $Z \rightarrow \pm\infty$  and hence cannot solve the normalization condition.  $A_1$  becomes the normalization constant and it is found by using eq.(7.48).

$$\int_{-\infty}^0 f^{(0)}(\alpha_n^{Z<0}(Z))^2 dZ + \int_0^{\infty} f^{(0)}(\alpha_n^{Z>0}(Z))^2 dZ = 1 \quad (7.55)$$

$$f^{(0)} \left( \int_0^{\infty} (\alpha_n^{Z<0}(-Z))^2 dZ + \int_0^{\infty} (\alpha_n^{Z>0}(Z))^2 dZ \right) = 1 \quad (7.56)$$

$$f^{(0)} A_1^2 \left( J_1^2(\sqrt{\lambda_n}) - J_0(\sqrt{\lambda_n}) J_2(\sqrt{\lambda_n}) \right) = 1 \quad (7.57)$$

$$\Rightarrow A_1 = \frac{1}{\sqrt{f^{(0)}}} \frac{1}{\sqrt{(J_1^2(\sqrt{\lambda_n}) - J_0(\sqrt{\lambda_n}) J_2(\sqrt{\lambda_n}))}} \quad (7.58)$$

One could claim that the general solution could be recovered from (7.53) by changing  $Z \rightarrow |Z|$ . However, in doing so, we force all the solutions to be even in  $Z$  and this new solution might not solve the differential equation anymore because of the discontinuity of  $|Z|$  at  $Z = 0$ . In order to obtain both odd and even functions, we consider  $\lambda_n$  as an explicit variable of the eigenfunctions ( $\alpha_n^{Z>0}(Z) = \alpha_n^{Z>0}(Z, \lambda_n)$ )

and find the set of values for  $\lambda_n$  that solve each of the following two conditions.

$$\alpha_n(0, \lambda_n) = 0 \quad (\text{Odd functions}) \quad (7.59)$$

$$\partial_Z \alpha_n(0, \lambda_n) = 0 \quad (\text{Even functions}) \quad (7.60)$$

When  $\alpha_n^{Z>0}(Z, \lambda_n)$  solves the first equation, we label it as odd, since this condition is a generic property of odd functions. Similarly, when  $\alpha_n^{Z>0}(Z, \lambda_n)$  solves the second equation, we label it as even since this condition is a generic property of even functions. The reason the eigenfunctions are labelled even/odd and not truly even/odd is because their behavior for  $Z < 0$  hasn't been determined yet. The even/oddness is resolved below. The next two graphs show the behavior of  $\alpha_n(0, \lambda_n) = A_1 J_1(\sqrt{\lambda_n})$  and  $\partial_Z \alpha_n(0, \lambda_n) = A_1 J_0(\sqrt{\lambda_n})$ . To graph these solutions we set  $f^{(0)} = 1$  since this constant is common to all solutions.

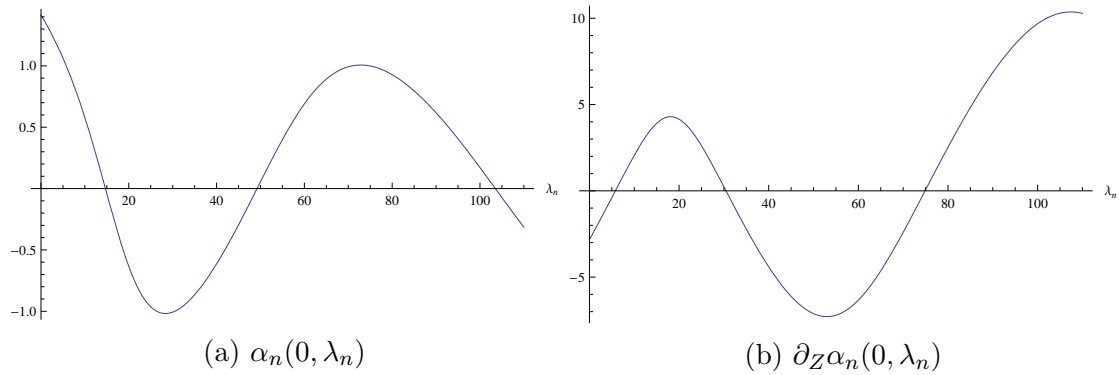


Figure 7-1: Zeroes of  $\alpha_n(0, \lambda_n)$  and  $\partial_Z \alpha_n(0, \lambda_n)$ .

The eigenvalues that solve one of the above conditions are listed below and can be easily read from the graphs.

Table 7–1: Zeroth-order eigenvalues of the six lightest vector mesons in the MDGJ model.

$\lambda_n^{(0)}$	Value	Even/Oddness
$\lambda_1^{(0)}$	5.78	Even
$\lambda_2^{(0)}$	14.68	Odd
$\lambda_3^{(0)}$	30.47	Even
$\lambda_4^{(0)}$	49.22	Odd
$\lambda_5^{(0)}$	74.89	Even
$\lambda_6^{(0)}$	103.50	Odd

#### 7.4.2 Zeroth-Order Eigenfunctions

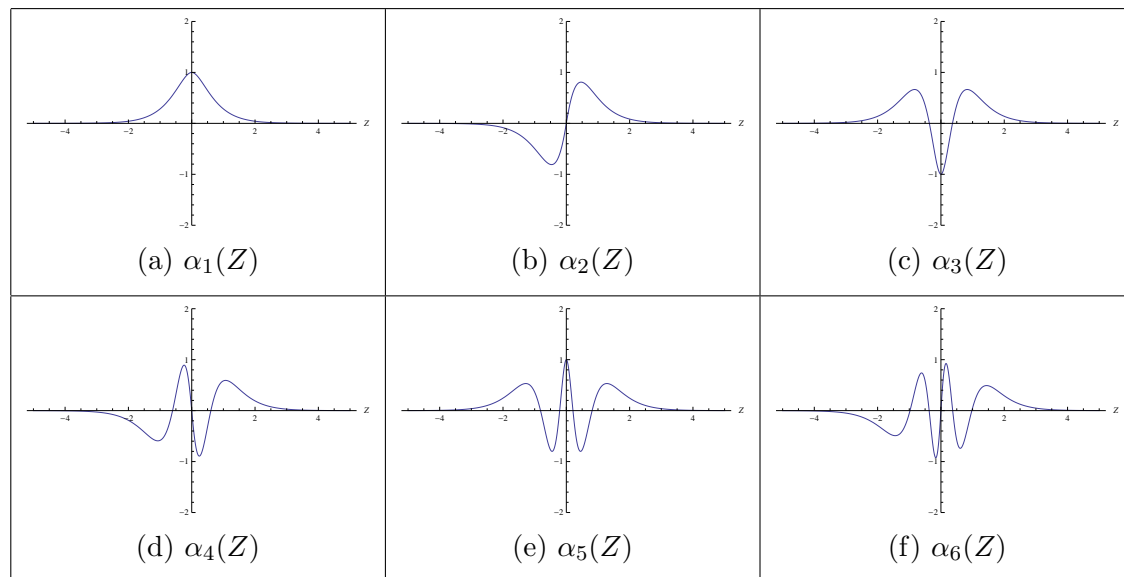
The odd-indexed solutions are even functions of  $Z$  and the even-indexed solutions are odd functions of  $Z$  as in the Sakai-Sugimoto model. Once the eigenvalues are found, we determine an appropriate behavior for  $\alpha_n(Z)$  in the range  $Z < 0$  such that it exhibits true evenness/oddness and solves eq. (7.52) for  $\alpha_n(Z) < 0$ . In the case of even eigenfunctions, we simply replace  $Z \rightarrow |Z|$ . In the case of odd eigenfunctions, we also replace  $Z \rightarrow |Z|$  and add an overall  $\text{sign}(Z)$  function which ensures the oddness of  $\alpha_n(Z)$ . Note that this extra  $\text{sign}(Z)$  doesn't change the normalization constant. Indeed, in the integral that defines the normalization equation, an additional  $(\text{sign}(Z))^2$  appears which is always equal to 1 except at one point ( $Z = 0$ ). Hence, the result of the integral doesn't change. The final solutions are summarized

as follows and are graphed using their respective  $\lambda_n$ .

$$\alpha_n^{\text{Even}}(Z) = \begin{cases} A_1 e^{-Z} J_1(\sqrt{\lambda_n} e^{-Z}) & Z \geq 0 \\ A_1 e^Z J_1(\sqrt{\lambda_n} e^Z) & Z < 0 \end{cases} \quad (n \in 2\mathbb{Z} + 1) \quad (7.61)$$

$$\alpha_n^{\text{Odd}}(Z) = \begin{cases} A_1 e^{-Z} J_1(\sqrt{\lambda_n} e^{-Z}) & Z \geq 0 \\ -A_1 e^Z J_1(\sqrt{\lambda_n} e^Z) & Z < 0 \end{cases} \quad (n \in 2\mathbb{Z}) \quad (7.62)$$

Figure 7-2: Zeroth-order eigenfunctions of the six lightest vector mesons in the MDGJ model.



As we can see in the plots above, the even-indexed functions are truly odd after adding the extra  $\text{sign}(Z)$ . Notice as well that the even and odd solutions are  $C^1$  functions, since the second derivative of the odd functions fail to be continuous at  $Z = 0$ . One has to fix the value of this second derivative to 0 ( $\partial_Z^2 \alpha_n^{\text{Odd}}(0) \equiv 0$ ) in

order to solve the differential equation (7.52) at  $Z = 0$ . Consequently, both odd and even functions solve the eigenvalue equation for all values of  $Z$ .

Also, with the eigenfunctions given in terms of Bessel functions, we obtain perfect orthogonality between two different solutions. First, by introducing this extra  $\text{sign}(Z)$  in odd-labelled functions, one automatically obtains orthogonality between odd and even functions since the integral of the orthogonality condition has a symmetric range ( $-\infty$  to  $\infty$ ). Orthogonality between two odd or two even functions is also achieved by looking at the result of the integral in such cases.

$$\begin{aligned} \langle \alpha_m^{(0)} | \alpha_n^{(0)} \rangle^{(0)} &= \int_{-\infty}^{\infty} dZ f^{(0)}(Z) \alpha_m^{(0)}(Z) \alpha_n^{(0)}(Z) \quad (m \neq n, (m, n) \in 2\mathbb{Z} \text{ or } 2\mathbb{Z} + 1) \\ &= \frac{2}{\lambda_m - \lambda_n} \left( \sqrt{\lambda_n} J_0(\sqrt{\lambda_n}) J_1(\sqrt{\lambda_m}) - \sqrt{\lambda_m} J_0(\sqrt{\lambda_m}) J_1(\sqrt{\lambda_n}) \right) \end{aligned} \quad (7.63)$$

When  $m$  and  $n$  are even, the functions are odd and solve eq.(7.59) implying that  $J_1(\sqrt{\lambda_n}) = J_1(\sqrt{\lambda_m}) = 0$ . On the other hand, when  $m$  and  $n$  are odd, the functions are even and solve eq.(7.60), i.e.,  $J_0(\sqrt{\lambda_n}) = J_0(\sqrt{\lambda_m}) = 0$ . The fact that we obtained a complete set of eigenfunctions with a general orthogonality condition that is satisfied for all eigenfunctions is no surprise. Indeed, the differential equation (7.52) can be cast into a Sturm-Liouville problem, which guarantees the existence of a complete set of orthonormal eigenfunctions.

### 7.4.3 First-Order Eigenvalue

We now assess the 1<sup>st</sup> order correction to the eigenvalues of eq.(7.47). The formula for such correction is well known in the literature.

$$\lambda_n^{(1)} = \langle \alpha_n^{(0)} | \mathbf{H}_v^{(1)} | \alpha_n^{(0)} \rangle^{(0)} \quad (7.64)$$

$$\text{with } \mathbf{H}_v^{(1)} = \frac{3 e^{2|Z|}}{2\pi} (|Z| \partial_Z^2 - 6 Z \partial_Z) \quad (7.65)$$

After operating  $\mathbf{H}_v^{(1)}$  and identifying  $|Z|'$ ,  $|Z|''$  with  $\text{sign}(Z)$ ,  $2 \delta(Z)$  respectively, the integral evaluates to the following expression.

$$\lambda_n^{(1)} = \frac{3}{2\pi (J_1^2(\sqrt{\lambda_n}) - J_0(\sqrt{\lambda_n}) J_2(\sqrt{\lambda_n}))} \left[ 2\lambda_n {}_3F_4 \left( 1, 1, \frac{3}{2}; 2, 2, 2, 2; -\lambda_n \right) \right. \\ \left. 1 - (1 + \lambda_n) J_0^2(\sqrt{\lambda_n}) - \lambda_n J_1^2(\sqrt{\lambda_n}) + \sqrt{\lambda_n} J_0(\sqrt{\lambda_n}) J_1(\sqrt{\lambda_n}) \right] \quad (7.66)$$

${}_3F_4$  is a generalized hypergeometric function and  $\lambda_n$  stands for the 0<sup>th</sup> order eigenvalue  $\lambda_n^{(0)}$ .

### 7.4.4 Field Identification

We would like to verify if this effective model of QCD shares even more similarities with the Sakai-Sugimoto model by comparing ratios of  $m_n^2$  of well-known fields. In order to do so, we must first identify which kind of meson fields are present in this effective theory by looking at their behavior under charge conjugation ( $\mathcal{C}$ ) and parity ( $\mathcal{P}$ ).

First of all, we determine the eigenvalue ( $\omega_{\mathcal{P},n} = \pm 1$ ) of the vector mesons  $B_\mu^{(n)}$  upon action of the parity operator. In the 5-dimensional theory, the parity operator

is a Lorentz transformation which flips the sign of spacelike coordinates.

$$\mathcal{P}(x^0, x^1, x^2, x^3, Z) = (x^0, -x^1, -x^2, -x^3, -Z) \quad (7.67)$$

Looking at the expansion of the four-dimensional gauge potential (7.23), we conclude that  $B_\mu^{(n)}$  must be odd (resp. even) under parity when  $\alpha_n$  is even (resp. odd) in order for  $A_\mu$  to behave as a 4-vector.

Second of all, the charge conjugation eigenvalue ( $\omega_{\mathcal{C},n} = \pm 1$ ) is determined with a similar logic. From the point of view of the string theory, vector mesons are built from quarks which correspond to modes of strings stretched between D4 and D6-branes (q) or D4 and  $\overline{\text{D6}}$ -branes ( $\bar{q}$ ). Since the D6 and  $\overline{\text{D6}}$  branes are antipodal on the  $\psi$  cycle, by changing  $\psi \rightarrow -\psi$  (or  $Z \rightarrow -Z$ ) we interchange the position of the D6 and  $\overline{\text{D6}}$  branes, which corresponds to changing the chirality of quarks in the effective QCD model. Hence, charge conjugation of the QCD model corresponds to a flip of the  $Z$  coordinate. Looking again at eq. (7.23), this means that  $B_\mu^{(n)}$  must be odd (resp. even) under charge conjugation when  $\alpha_n$  is even (resp. odd) in order for  $A_\mu$  to acquire an overall sign under charge conjugation as expected.

Knowing the eigenvalues of each vector mesons under  $\mathcal{P}$  and  $\mathcal{C}$ , we can identify them easily using the Particle Data Group (PDG) database [16] where we use their mass measurements  $M_{\text{PDG}}$  for comparison. Also, we specify to fields that are vectors of the approximate isospin  $SU(2)$  symmetry as clarified in [51].

### 7.4.5 Comparison of the Mass Ratios

We first summarize our knowledge of each vector mesons  $B_\mu^{(n)}$ .

Table 7–2: Vector mesons of the MDGJ model.

	$\lambda_n^{(0)}$	$\omega_{\mathcal{C}}$	$\omega_{\mathcal{P}}$	PDG name	$M_{\text{PDG}}(\text{MeV})$
$B_\mu^{(1)}$	5.78	+	+	$\rho(770)$	775.49
$B_\mu^{(2)}$	14.68	-	-	$a_1(1260)$	1230
$B_\mu^{(3)}$	30.47	+	+	$\rho(1450)$	1465
$B_\mu^{(4)}$	49.22	-	-	$a_1(1640)$	1647
$B_\mu^{(5)}$	74.89	+	+	$\rho(1700)$	1720

By taking the zeroth and first-order eigenvalues into account, we predict the squared-mass ratios using this formula:

$$R_{n/m} \equiv \frac{\lambda_n}{\lambda_m} = \frac{\lambda_n^{(0)} + \delta \lambda_n^{(1)} + O(\delta^2)}{\lambda_m^{(0)} + \delta \lambda_m^{(1)} + O(\delta^2)} \approx \frac{\lambda_n^{(0)}}{\lambda_m^{(0)}} + \frac{\delta}{\left(\lambda_m^{(0)}\right)^2} \left(\lambda_m^{(0)} \lambda_n^{(1)} - \lambda_n^{(0)} \lambda_m^{(1)}\right) \quad (7.68)$$

We stop at first-order terms in the  $\delta$  expansion, since our analysis hasn't considered contributions from higher orders.

In order to obtain numerical estimates for  $R_{n/m}$ , we determine the arbitrary parameter  $\delta$  in two ways. For each of these ways of fixing  $\delta$ , we present a summary table of our predictions for  $R_{n/1}$  compared with the estimates of the Sakai-Sugimoto model and the PDG value  $R_{n/1}^{\text{PDG}}$ . We took care to number our eigenvalues in the

same way as Sakai & Sugimoto to facilitate comparison. The second column of each of these tables informs the reader about the eigenvalue ratio corresponding to the given squared-mass ratio. The fourth column presents our zeroth-order estimates of the ratios, symbolized as  $R_{n/m}^{(0)} \equiv \frac{\lambda_n^{(0)}}{\lambda_m^{(0)}}$ , in order to see the effect of the  $\delta$  correction.

1. We determine  $\delta = 0.042713$  by fixing the first ratio  $R_{2/1}$  to its experimental value.

Table 7–3: MDGJ vs Sakai-Sugimoto predictions determining  $\delta$  by fixing  $R_{2/1}$ .

	$\lambda_n/\lambda_m$	Sakai-Sugimoto	MDGJ		Exp. Value $R_{n/m}^{\text{PDG}}$
			$R_{n/m}^{(0)}$	$R_{n/m}$	
$m_{a_1(1260)}^2/m_{\rho(770)}^2$	$\lambda_2/\lambda_1$	2.32	2.54	2.52	2.52
$m_{\rho(1450)}^2/m_{\rho(770)}^2$	$\lambda_3/\lambda_1$	4.22	5.27	5.14	3.57
$m_{a_1(1640)}^2/m_{\rho(770)}^2$	$\lambda_4/\lambda_1$	6.62	8.51	8.23	4.51
$m_{\rho(1700)}^2/m_{\rho(770)}^2$	$\lambda_5/\lambda_1$	9.53	12.95	12.42	4.92

2. We determine  $\delta = 0.642752$  by minimizing the  $\chi^2$  associated to the vector mesons ratios. We minimize  $\chi^2/3$  to 2.77 while Sakai & Sugimoto obtain  $\chi^2/3 = 650.03$ .

Table 7–4: MDGJ vs Sakai-Sugimoto predictions determining  $\delta$  by minimizing the vector mesons  $\chi^2$ .

	$\lambda_n/\lambda_m$	Sakai-Sugimoto	MDGJ		Exp. Value $R_{n/m}^{\text{PDG}}$
			$R_{n/m}^{(0)}$	$R_{n/m}$	
$m_{a_1(1260)}^2/m_{\rho(770)}^2$	$\lambda_2/\lambda_1$	2.32	2.54	2.21	2.52
$m_{\rho(1450)}^2/m_{\rho(770)}^2$	$\lambda_3/\lambda_1$	4.22	5.27	3.39	3.57
$m_{a_1(1640)}^2/m_{\rho(770)}^2$	$\lambda_4/\lambda_1$	6.62	8.51	4.36	4.51
$m_{\rho(1700)}^2/m_{\rho(770)}^2$	$\lambda_5/\lambda_1$	9.53	12.95	5.04	4.92

Looking at the results of table 7–3, we conclude that the  $\delta$  corrections of the MDGJ model decrease the value of the zeroth-order ratios reducing the gap with the PDG values. However, the corrections are not significant enough to obtain values better than Sakai-Sugimoto’s predictions.

Regarding the results of table 7–4, the MDGJ ratios are in general closer to the experimental values than Sakai-Sugimoto’s predictions. Although the correction of the first ratio worsens the gap with the experimental value, the MDGJ model has a much better  $\chi^2/\text{DOF}$  than Sakai-Sugimoto. However, one might argue that the derived value of  $\delta$  is too close to 1 to guarantee a good perturbation expansion. The

significant first-order corrections for the third and fourth ratios might destroy the good fit once one considers the second-order terms.

## CHAPTER 8

### Conclusion

The goal of this thesis was to provide detailed calculations of the masses of mesonic fields emerging in the MDGJ model. First, we performed a T-duality of the MDGJ model in order to compare the structure of the gravity theory with the one suggested by Sakai and Sugimoto. This comparison showed several similarities, which motivated us to use their method for calculating the mesonic masses. We analyzed the DBI action of the probe D6-branes in a background of D4-branes after embedding the probe branes at antipodal points on the compact  $\psi$  cycle of the conifold. We then considered the gauge flux on the D6-branes to be a function of the Minkowski coordinates and  $Z$  only, knowing that dependence on the internal conifold coordinates would modify the symmetry of the resulting four-dimensional Yang-Mills theory.

To reduce the dimensions of the action down to four dimensions, we separated the Minkowski coordinates from the  $Z$  coordinate by expanding the gauge flux with a complete set of functions of  $Z$ . This led us to a QCD-like action provided that we would fix the coefficients of the terms of this action to their typical values. This was done by imposing a specific eigenvalue equation on the complete set of functions of  $Z$  and the eigenvalue of each of these eigenfunctions determined the mass of the associated meson field.

In the large  $N$  limit, we used  $\delta = g_s M^2/N$  as a small parameter, which we used to control the estimates of the eigenvalues and eigenfunctions. Consequently, we provided the zeroth and first-order approximations of the eigenvalues with which we made predictions for the ratios of squared-masses. Our results showed better agreement than Sakai-Sugimoto compared to the experimental values when we fixed  $\delta$  by minimizing the  $\chi^2/\text{DOF}$ .

For future directions, one could clarify how the chiral symmetry breaking emerges from the gravity theory point of view. This is an important aspect of QCD, which hasn't been explained in the MDGJ model. One could also retrieve a KSRF-type relation between the pion and vector mesons couplings, which would show similitudes with the local symmetry approach initiated by Georgi. Moreover, Sakai and Sugimoto found scalar mesons by considering fluctuations of the orthogonal direction of the D8-branes. This led to scalar fields in the reduced four-dimensional action and their associated mass was found by using a method similar to the one used in the vector meson calculations. By fluctuating the D6-brane  $Y$  coordinate in the MDGJ model, one could also obtain scalar mesons along with their associated mass value.

## References

- [1] O. Aharony, S. Gubser, J. Maldacena, H. Ooguri, and Y. Oz, “Large N Field Theories, String Theory and Gravity,” May 1999, hep-th/9905111.
- [2] M. Mia, K. Dasgupta, C. Gale, and S. Jeon, “Toward Large N Thermal QCD from Dual Gravity: The Heavy Quarkonium Potential,” April 2010, 1004.0387.
- [3] G. 't Hooft, “A planar diagram theory for strong interactions,” *Nuclear Physics B*, vol. 72, no. 3, pp. 461 – 473, 1974.
- [4] J. M. Maldacena, “The Large N Limit of Superconformal Field Theories and Supergravity,” November 1997, hep-th/9711200.
- [5] C. P. Herzog, “Lectures on Holographic Superfluidity and Superconductivity,” *J. Phys. A*, vol. 42, April 2009, 0904.1975.
- [6] S. Ryu and T. Takayanagi, “Aspects of Holographic Entanglement Entropy,” May 2006, hep-th/0605073.
- [7] P. Kovtun, D. Son, and A. Starinets, “Viscosity in Strongly Interacting Quantum Field Theories from Black Hole Physics,” May 2004, hep-th/0405231.
- [8] M. Luzum and P. Romatschke, “Conformal Relativistic Viscous Hydrodynamics: Applications to RHIC results at  $\sqrt{s_N N} = 200$  GeV,” *Phys. Rev. C.*, vol. 78, April 2008, 0804.4015.
- [9] M. Kruczenski, D. Mateos, R. C. Myers, and D. J. Winters, “Towards a holographic dual of large- $N_c$  QCD,” September 2004, hep-th/0311270.
- [10] T. Sakai and S. Sugimoto, “Low energy hadron physics in holographic QCD,” *Prog.Theor.Phys.*, vol. 113, pp. 843–882, December 2004, hep-th/0412141.
- [11] M. Mia, K. Dasgupta, C. Gale, and S. Jeon, “Five Easy Pieces: The Dynamics of Quarks in Strongly Coupled Plasmas,” February 2009, 0902.1540.

- [12] M. E. Peskin and D. V. Schroeder, *An Introduction To Quantum Field Theory (Frontiers in Physics)*. Westview Press, 1995.
- [13] C. Burgess and G. Moore, *The Standard Model: A Primer*. Cambridge University Press, December 2006.
- [14] M. Srednicki, *Quantum Field Theory*. Cambridge University Press, Janvier 2007.
- [15] J. Goldstone, “Field Theories with Superconductor Solutions,” *Nuovo Cim.*, vol. 19, pp. 154–164, 1961.
- [16] Regents of the University of California, “The Particle Data Group.”
- [17] D. J. Gross and F. Wilczek, “Ultraviolet Behavior of Non-Abelian Gauge Theories,” *Phys. Rev. Lett.*, vol. 30, pp. 1343–1346, June 1973.
- [18] H. D. Politzer, “Reliable Perturbative Results for Strong Interactions?,” *Phys. Rev. Lett.*, vol. 30, pp. 1346–1349, June 1973.
- [19] M. B. Green, J. Schwarz, and E. Witten, *Superstring Theory*, vol. 1-2. Cambridge University Press, 1987.
- [20] J. Polchinski, *String Theory*, vol. 1-2. Cambridge University Press, October 1998.
- [21] K. Becker, M. Becker, and J. H. Schwarz, *String Theory and M-Theory: A Modern Introduction*. Cambridge University Press, January 2007.
- [22] E. Kiritsis, *String Theory in a Nutshell*. Princeton University Press, March 2007.
- [23] E. Cremmer, B. Julia, and J. Scherk, “Supergravity Theory in Eleven-Dimensions,” *Phys.Lett.*, vol. B76, pp. 409–412, 1978.
- [24] J. H. Schwarz, “Covariant Field Equations of Chiral N=2 D=10 Supergravity,” *Nucl.Phys.*, vol. B226, p. 269, 1983.
- [25] Y. Kim, I. J. Shin, and T. Tsukioka, “Holographic QCD: Past, Present, and Future,” May 2012, 1205.4852.
- [26] E. Witten, “Bound states of strings and p-branes,” *Nucl.Phys.*, vol. B460, pp. 335–350, 1996, hep-th/9510135.

- [27] S. T. Yau, “Calabi’s conjecture and some new results in algebraic geometry,” *Proc. Nat. Acad. Sci. U.S.A.*, vol. 74, no. 5, pp. 1798–1799, 1977.
- [28] T. Buscher, “A Symmetry of the String Background Field Equations,” *Phys.Lett.*, vol. B194, p. 59, 1987.
- [29] E. Bergshoeff, C. M. Hull, and T. Ortin, “Duality in the type II superstring effective action,” *Nucl.Phys.*, vol. B451, pp. 547–578, 1995, hep-th/9504081.
- [30] B. Zwiebach, *A First Course in String Theory*. Cambridge University Press, January 2009.
- [31] J. Polchinski, “Dirichlet-Branes and Ramond-Ramond Charges,” *Phys. Rev. Lett.*, vol. 75, October 1995, hep-th/9510017.
- [32] S. Sugimoto and K. Takahashi, “QED and String Theory,” March 2004, hep-th/0403247.
- [33] H. Georgi, “New realization of chiral symmetry,” *Phys. Rev. Lett.*, vol. 63, pp. 1917–1919, Oct 1989.
- [34] H. Georgi, “Vector realization of chiral symmetry,” *Nuclear Physics B*, vol. 331, no. 2, pp. 311 – 330, 1990.
- [35] K. Kawarabayashi and M. Suzuki, “Partially Conserved Axial-Vector Current and the Decays of Vector Mesons,” *Phys. Rev. Lett.*, vol. 16, pp. 255–257, Feb 1966.
- [36] Riazuddin and Fayyazuddin, “Algebra of Current Components and Decay Widths of  $\rho$  and  $K^*$  Mesons,” *Phys. Rev.*, vol. 147, pp. 1071–1073, Jul 1966.
- [37] O. Aharony, J. Sonnenschein, and S. Yankielowicz, “A holographic model of deconfinement and chiral symmetry restoration,” *Annals Phys*, vol. 322, pp. 1420–1443, April 2006, hep-th/0604161.
- [38] G. Mandal and T. Morita, “Gregory-Laflamme as the confinement/deconfinement transition in holographic QCD,” July 2011, 1107.4048.
- [39] R. Gregory and R. Laflamme, “The Instability of Charged Black Strings and p-Branes,” *Nuclear Physics B*, vol. 428, pp. 399–434, April 1994, hep-th/9404071.

- [40] F. Chen, L. Chen, K. Dasgupta, M. Mia, and O. Trottier, “A UV complete model of Large N Thermal QCD,” *Phys. Rev. D.*, vol. 87, p. 041901, 09 2012, 1209.6061.
- [41] I. R. Klebanov and M. J. Strassler, “Supergravity and a Confining Gauge Theory: Duality Cascades and  $\chi$  SB-Resolution of Naked Singularities,” *JHEP*, vol. 052, p. 0008, July 2000, hep-th/0007191.
- [42] P. Candelas and X. C. de la Ossa, “Comments on conifolds,” *Nuclear Physics B*, vol. 342, no. 1, pp. 246 – 268, 1990.
- [43] M. Mia and F. Chen, “Non extremal geometries and holographic phase transitions,” *JHEP*, vol. 1301, p. 083, 2013, 1210.3365.
- [44] I. R. Klebanov and N. A. Nekrasov, “Gravity duals of fractional branes and logarithmic RG flow,” *Nucl.Phys.*, vol. B574, pp. 263–274, 2000, hep-th/9911096.
- [45] P. Ouyang, “Holomorphic D7-Branes and Flavored N=1 Gauge Theories,” *Nucl.Phys.B*, vol. 699, pp. 207–225, 05 2004, hep-th/0311084.
- [46] M. J. Strassler, “The Duality Cascade,” May 2005, hep-th/0505153.
- [47] H. Ooguri and C. Vafa, “Summing up D-Instantons,” *Phys. Rev. Lett.*, vol. 77, pp. 3296–3298, August 1996, hep-th/9608079.
- [48] K. Dasgupta and S. Mukhi, “Brane Constructions, Conifolds and M-Theory,” *Nuclear Physics B*, vol. 551, pp. 204–228, November 1998, hep-th/9811139.
- [49] K. Dasgupta, P. Franche, A. Knauf, and J. Sully, “D-terms on the resolved conifold,” *JHEP*, vol. 027 (2009), p. 0904, February 2008, 0802.0202.
- [50] L. Chen, K. Dasgupta, C. Gale, M. Mia, M. Richard, and O. Trottier, *To Appear*. 2013.
- [51] D. Son and M. Stephanov, “QCD and dimensional deconstruction,” *Phys. Rev. D.*, vol. 69 (2004), April 2003, hep-ph/0304182.